HHS Public Access

Author manuscript

Circ Res. Author manuscript; available in PMC 2017 September 02.

Published in final edited form as:

Circ Res. 2016 September 2; 119(6): 731–750. doi:10.1161/CIRCRESAHA.116.308422.

Knock Down of Plakophilin 2 Downregulates miR-184 Through CpG Hypermethylation and Suppression of the E2F1 Pathway and Leads to Enhanced Adipogenesis In Vitro

Priyatansh Gurha, **Xiaofan Chen**, **Raffaella Lombardi**, **James T. Willerson**, and **AJ Marian**

Center for Cardiovascular Genetics, Institute of Molecular Medicine and Department of Medicine, University of Texas Health Sciences Center at Houston, and Texas Heart Institute, Houston, TX 77030

Abstract

Rationale—*PKP2*, encoding plakophilin 2 (PKP2), is the most common causal gene for arrhythmogenic cardiomyopathy (AC).

Objective—To characterize miRNAs expression profile in PKP2-deficient cells

Methods and Results—Control and PKP2-knock down HL-1 (HL-1$^{Pkp2\text{-}shRNA}$) cells were screened for 750 miRNAs using low-density microfluidic panels. Fifty-nine miRNAs were differentially expressed. MiR-184 was the most down-regulated miRNA. Expression of miR-184 in the heart and cardiac myocyte was developmentally downregulated and was low in mature myocytes. MicroRNA-184 was predominantly expressed in cardiac mesenchymal progenitor cells (MPCs). Knock down of *Pkp2* in cardiac MPCs also reduced miR-184 levels.

Expression of miR-184 was transcriptionally regulated by the E2F1 pathway, which was suppressed in PKP2-deficient cells. Activation of E2F1, upon over-expression of its activator CCND1 or knock down of its inhibitor RB1, partially rescued miR-184 levels. In addition, DNMT1 was recruited to the promoter region of miR-184 and the CpG sites at the upstream region of miR-184 were hypermethylated. Treatment with 5-aza-2'-deoxycytidine, a demethylation agent, and knock down of DNMT1 partially rescued miR-184 level. Pathway analysis of paired miR-184:mRNA targets identified cell proliferation, differentiation, and death as the main affected biological processes. Knock down of miR-184 in HL-1 cells and MPCs induced and conversely, its over-expression attenuated adipogenesis.

Conclusions—PKP2 deficiency leads to suppression of the E2F1 pathway and hypermethylation of the CpG sites at miR-184 promoter, resulting in downregulation of miR-184 levels. Suppression of miR-184 enhances and its activation attenuates adipogenesis in vitro. Thus, miR-184 contributes to the pathogenesis of adipogenesis in PKP2-deficient cells.

Address correspondence to: Dr. AJ Marian, Center for Cardiovascular Genetics, 6770 Bertner Street, Suite C900A, Houston, TX 77030, 713 500 2350, Ali.J.Marian@uth.tmc.edu, Dr. Priyatansh Gurha, Center for Cardiovascular Genetics, 6770 Bertner Street, Suite C905, Houston, TX 77030, 713 500 2335, Priyatansh.Gurha@uth.tmc.edu.

P.G., and X.C. are co-first authors.

DISCLOSURE

None.

Keywords

MicroRNA; epigenetics; DNA methylation; heart failure; cardiomyopathy; gene expression

INTRODUCTION

Arrhythmogenic Cardiomyopathy (AC) is a hereditary cardiomyopathy that manifests with ventricular arrhythmias, sudden cardiac death (SCD), and heart failure [1, 2]. The pathological hallmark of AC is a gradual and progressive replacement of cardiac myocytes by fibro-adipocytes, which classically shows a predilection toward involvement of the right ventricle, and hence, the term arrhythmogenic right ventricular cardiomyopathy (ARVC) [3, 4]. AC is an enigmatic disease with an inadequately understood pathogenesis. Recent molecular genetic discoveries have led to partial elucidation of the causal genes and identification of mutations in genes encoding the protein constituents of the intercalated disks (IDs) [5-9]. IDs are cell-cell adhesion structures composed of desmosomes, adherens junctions, and the gap junctions. IDs not only provide mechanical integrity to the myocardium but also control contact-regulated signal transduction [10]. Mutations in Lamin A/C (LMNA) and transmembrane protein 43 (TMEM43) are also associated with AC [11, 12]. Overall, *PKP2* gene encoding plakophilin 2 (PKP2), a constituent of the IDs, is the most common causal gene for AC [13, 14].

The molecular links between the mutant causal proteins and the ensuing cardiac phenotype in AC are not fully known. Extensive molecular remodeling of the IDs in AC impairs mechano-transduction and is associated with activation of the Hippo pathway, a contact-regulated signaling pathway involved in cellular growth, differentiation and proliferation [15]. Activation of the Hippo pathway results in suppression of gene expression through its downstream effector, the YAP-TEAD complex as well as suppression of the canonical Wnt signaling through the β catenin (CTNNB1)-TCF7L2 transcriptional machinery [15-17]. Collectively, these cell-signaling events impart transcriptional changes that regulate cell growth, proliferation, and differentiation, leading to phenotypic expression of AC [15].

MicroRNAs (miRNAs) are small 22 nucleotide molecules that regulate gene expression and impact various biological processes, including cardiac hypertrophy, myocytes differentiation, and proliferation. [18-20]. MiRNAs are largely “nudgers and tweakers of genome management” as their effects on transcript levels, by-and-large, are modest [21]. Because of multiplicity of their targets, however, miRNAs influence various molecular networks and biological processes [20, 22-30]. MiRNAs are also targets of various signaling pathways, including Hippo and the canonical Wnt pathways, which are implicated in AC [20, 22-2930]. Moreover, miRNAs are implicated in the pathogenesis of heart failure, fibrosis and adipogenesis [18, 31-33], phenotypes typically observed in patients with cardiomyopathies [2-4]. Thus, we hypothesized that miRNAs are also involved in the pathogenesis of AC. To test this hypothesis, we screened for the differentially expressed miRNAs and characterized functional and biological effects of the most down-regulated miRNA in HL-1 and cardiac mesenchymal progenitor cells.

METHODS

An expanded version of Material and Methods is provided as Online Supplementary Material.

Recombinant viral constructs

Recombinant lentiviruses were generated as published [15]. The miR-Zip vector contained shRNAs positioned in tandem with a GFP expression cassette downstream to an H1 promoter. MiR-184 over-expression vector contained a 500bp genomic fragment of miR-184 in the miR-Express vector. Commercially available lentiviruses expressing shRNAs against target transcripts and pre-packaged recombinant adenoviral constructs were used. HL-1 cells at 70-90% confluence were transduced with the recombinant viruses. Transduction efficiency was determined by detecting the GFP signal under fluorescence microscopy, FACS analysis, and quantification of the target transcript levels.

Suppression of expression of PKP2 in the HL-1 cells

Two independent PKP2-deficient HL-1 lines (HL-$1^{Pkp2\text{-}shRNA}$) were established using two different shRNAs, as published [15]. Knock down of *Pkp2* mRNA and PKP2 protein levels were detected by qPCR and immunoblotting (IB), respectively.

Isolation of cardiac myocytes and mesenchymal progenitor cells (MPCs)

To isolate cardiac myocytes explanted hearts were perfused with a Ca^{2+} free perfusion buffer and subjected to digestion in a collagenase buffer. Myocytes were dissociated and gravity precipitated in the presence of 200 mM ATP and centrifugation at 20 g. The isolated myocytes were re-introduced to increasing concentrations of calcium at a final concentration of 1.5 mM of CaCl2 and placed in culture dishes or cover glasses coated with laminin.

Cardiac MPCs were isolated by sorting of non-myocyte fraction of cardiac cells against anti CD44 and anti platelet-derived growth factor α (PDGFRA) antibodies, per published protocols [34-36].

Mouse models of AC

Myh6:Jup^{Tr} mice have been published [16, 37, 38]. To knock down *Pkp2* gene in the heart, an shRNA targeting the *Pkp2* mRNA (position 1154-1174) was cloned into the U6-LoxP-Neo vector [39, 40]. *Nkx2-5:Cre* deleter mice was used to remove a LoxP neo cassette and conditionally activate expression of the shRNA against *Pkp2* mRNA (*Pkp2*^{shRNA}) in the cardiogenic lineage [41].

MicroRNA expression profiling

Expression profile of miRNAs was determined using TaqMan low-density (TLDA) microfluidic cards (Rodent miRNA v3.0 Card A and Card B Applied Biosystems). The panels contain a total of 750 mature miRNAs of which 641 are annotated and curated in the mouse genome. Mouse small nucleolar RNA (*MammU6*) was used for data normalization and relative quantification, as it was spotted 3 times in each card, as opposed to other controls. In brief, aliquots of RNA isolated from the HL-1 and HL-$1^{Pkp2\text{-}shRNA}$ cells from

two independent experiments were reverse-transcribed into cDNAs and amplified by quantitative PCR (qPCR). MiRNAs with Ct values of greater than 35 were excluded.

IB and Immunofluorescence (IF) staining

IB and IF were performed per the conventional methods [15, 36]. The list of the primary and secondary antibodies used is provided in Online Table I.

In situ hybridization

In situ hybridization was performed per a published protocol [42]. In brief, thin myocardial sections were hybridized with a 5' and 3' dual DIG-labeled detection probe against miR-184 or a control scrambled probe. Sections were washed in PBS following overnight hybridization, mounted, and examined under light microscopy.

Quantitative PCR

Total RNA (including miRNA) was extracted and reverse transcribed. MiRNAs were amplified using specific TaqMan gene expression assays and TaqMan MicroRNA assays (Online Table I). *Gapdh* and *snoRNA202* transcript levels were used for normalization for mRNA and miRNA levels, respectively. $2^{\Delta\Delta Ct}$ method was used to calculate the normalized gene expression values.

MicroRNA targets and miRNA-mRNA pairing

Global gene expression patterns were determined by whole transcriptome sequencing (RNA-Seq), as published [15]. Predicted miR-184 targets were identified using miRWalk online software (www.umm.uni-heidelberg.de/apps/zmf/mirwalk/). Genes that were identified as targets in at least 2 different databases were analyzed. MiRNA-mRNA pairing was carried out using the Ingenuity Pathway Analysis (IPA) software (www.ingenuity.com). All putative targets of miR-184 were identified using the miRwalk and IPA software. Targets that were identified by at least 2 programs and had a seed length of 6 nucleotides or longer were included for further analyses. The candidate target mRNAs and differentially expressed mRNAs were matched and those mRNAs that had a minimum FPKM value of 1 in at least one sample and showed a reciprocal expression to its corresponding miRNA were considered as targets. Finally, target gene expression cutoff was set at 1.2 fold expression and the q value at 0.05. To examine the potential biological significance of paired changes, gene ontology over-representation analysis, upstream regulator, and canonical pathway analyses were performed using IPA.

Adiogenesis network analysis

A protein functional association network was constructed for miR-184 targets that were involved in adipogenesis, namely, AGPAT1, AGPAT3, NCOA1, and PPARGC1B using the STRING online tool. The medium confidence score for interaction was set at 0.4 and the option for all active prediction method was included. Direct interactions are depicted as colored nodes in the Network. Gene that are identified as members of the network and were found to be upregulated in the HL-$1^{Pkp2\text{-}shRNA}$ cells in RNA-seq data were further validated to build a miR-184 target network for adipogenesis.

Adipogenesis

Induction and quantification of adipogenesis in the HL-1 cells and MPCs cells were as described [15]. In brief, ~5 ×10^4 HL-1 cells or MPCs were treated with an adipogenesis induction medium for 7 to 14 days. Quantitative PCR and IB were used to quantify transcript and protein levels of selected genes that regulate adipogenesis, respectively. Accumulation of fat droplets was assessed by Oil Red O staining and expression of adipogenic transcription factors CEBPA, and PPARG expression by IF.

Activation and suppression of selected signaling pathways

To determine the effect of activation of the E2F signaling pathway on miR-184 levels, HL-1 cells were transduced with recombinant adenoviruses expressing CCND1. Likewise, a siRNA construct was used to target retinoblastoma (RB1), an inhibitor of E2F1 pathway. Control viruses and viruses expressing no-target (NT) or scrambled shRNAs and non-targeting siRNAs were included as controls.

To activate the canonical Wnt signaling, cells were treated with Wnt-3A at 40, 80, and 120 ng/mL for 24h. To suppress the canonical Wnt signaling pathway, HL-1 cells were transduced with recombinant lentiviruses expressing shRNA against *Tcf7l2* (Lenti:*Tcf7l2*^{shRNA}). Activation or suppression of the canonical Wnt signaling pathway was also confirmed by quantifying protein levels of TCF7L2, mRNA levels of *Axin2* and *Ccnd1* and by a *Tcf7l2*-luciferase reporter assay.

To activate gene expression through the Hippo pathway, HL-1 cells were treated with 1uM of 1-Oleoyl lysophophatidic acid (LPA) for 1, 2 and 4h. To suppress gene expression through the Hippo pathway, cells were transduced with the recombinant lentiviruses expressing an shRNA against *Yap* (Lenti: *Yap*^{shRNA}). Activity state of the Hippo pathway was confirmed by quantifying levels of YAP protein by IB, mRNA levels of target transcripts *Ctgf* and *Cry61* by qPCR and a TEAD luciferase assay.

DNA methylation assay

To determine whether suppression of miR-184 was a consequence of DNA methylation-dependent epigenetic silencing of the locus, the genomic sequence upstream of the pre-miR-184 transcription start site was analyzed for the presence of CpG rich regions. Using EMBOSS Cpgplot (http://www.ebi.ac.uk/Tools/seqstats/emboss_cpgplot/) 15 CpG sites with observed/expected ratio of > 0.60, located 500-800 bp upstream to the pre-miRNA start site, were identified. This region was used for DNA methylation analysis by bisulfite conversion, cloning and sequencing of individual clones. Genomic DNA was extracted from the HL-1 and HL-1$^{Pkp2\text{-}shRNA}$ cells, treated for bisulfite conversion, and PCR amplified using primers specific to the miR-184 upstream region (Online Table I). PCR products were cloned using a TA cloning strategy, and then sequenced. Methylation of CpG sites was analyzed using QUMA online tool (http://quma.cdb.riken.jp/).

To determine effects of DNA methylation, *Dnmt1* was knocked down using recombinant lentiviruses expressing respective shRNAs, as described above.

Statistics

Data were presented as mean ± SD. Differences in the continuous variables between the two groups were compared by t-test or Mann-Whitney U test and among multiple groups by one-way ANOVA. Whenever applicable, multiple groups Dunnett's corrected p values for pairwise comparisons were presented. Differences among the categorical values were compared by Kruskall-Wallis test. Statistical significance for methylation at each CpG sites was calculated by Fisher exact test (QUMA online tool).

RESULTS

Differentially expressed miRNAs in PKP2-deficient HL-1 (HL-1$^{Pkp2\text{-}shRNA}$) cells

Two independent lines of HL-1$^{Pkp2\text{-}shRNA}$ were generated using two different sets of shRNAs that target *Pkp2* transcript (Figure 1A). Quantitative PCR showed reduced *Pkp2* mRNA levels by 3.7±0.5 -fold (shRNA#1, N=6, p<0.001) and 2.4±0.4 -fold (shRNA#2, N=5, p<0.001), as compared to control HL-1 cells (Figure 1B). Likewise, PKP2 protein levels were reduced by 81.1±10.4% (shRNA#1, N=5, p<0.0001) and 77.8±15.6% (shRNA#2, N=5, p<0.0001), as compared to control cells (Figure 1C, D).

To identify differentially expressed miRNAs in the HL-1$^{Pkp2\text{-}shRNA}$ cells, miRNAs were screened using TLDA microfluidic panels comprising 641 unique miRNAs. A total of 292 miRNAs were expressed in the HL-1 cells at a threshold Ct value of ≤35. Thirty-one miRNAs were upregulated, 28 downregulated, and 233 were unchanged in the HL-1$^{Pkp2\text{-}shRNA}$ cells as compared to control HL-1 cells (Figure 1E, F, and Online Table II).

MiR-200b, miR-487b, and miR-429 were the most upregulated while miR-184 and miR-881 were the most downregulated miRNAs (Figure 1F). MiR-184, an independently transcribed miRNA, was the most down-regulated miRNA in both lines of HL-1$^{Pkp2\text{-}shRNA}$ cells (Figure 1E, F, and G). It was reduced by more by ~ 14-fold (N=24, p<0.0001). Likewise, transcript levels of miR-881 were reduced by 64.14±19.9% in the HL-1$^{Pkp2\text{-}shRNA}$ cells (p<0.0001). Quantitative PCR validation of top upregulated miRNAs showed miR-200b levels were increased by 7.99±0.27 (N=4, p<0.0001) and miR-429 by 7.98±0.37 (N=4, p<0.0001) in the HL-1$^{Pkp2\text{-}shRNA}$ cells (Figure 1H). Given robust and consistent down regulation of miR-184 levels in the PKP2-deficient HL-1 cells and in view of a paucity of data on the biological functions of miR-184 in the heart, it was further characterized.

Generation and characterization of an Nkx2.5-Cre:Pkp2^{shRNA} mouse model of AC

To extend the in vitro findings to in vivo models of AC, expression of *PKP2*, the most common causal gene for AC [13, 14], was conditionally knocked down in the mouse heart upon expression of an shRNA against *Pkp2* mRNA, under the transcriptional regulation of the *Nkx2-5* locus (Figure 2A). *Pkp2* mRNA and PKP2 protein levels were reduced by 41±10 % and 54±21%, respectively, in the *Nkx2.5*-Cre:*Pkp2*^{shRNA} mice, as compared to wild type mice (Figure 2B-D). The *Nkx2.5*-Cre:*Pkp2*^{shRNA} mice survived normally but exhibited significantly enlarged left ventricle and decreased cardiac systolic function (Online Table III). Right ventricular function could not be reliable evaluated by echocardiography. Interstitial fibrosis was increased by 2.1±1.2 -fold (Figure 2E, F). Likewise, the number of

cells accumulating fat droplets was increased by 5.1±3.5 -fold (N=7, p=0.037) in the hearts of *Nkx2.5*-Cre:*Pkp2*^{shRNA} mice (Figure 2G, H). The observed phenotype is similar to that in the previously described mouse models of AC [16, 37].

Suppressed miR-184 levels in independent mouse models of AC

Expression levels of miRNA-184 were determined by qPCR in the heart of the *Nkx2.5*-Cre:*Pkp2*^{shRNA}, and the *Myh6-Jup*^{Tr} mice [37]. Levels of miR-184 were reduced by 52±21 % in the hearts of 4-week old *Nkx2.5-Cre:Pkp2*^{shRNA} mice (Figure 2I, N=9, p=0.004) and by 49±10% (N=6, p=0.0048) in the hearts of *Myh6:Jup*^{Tr} mice, compared to age- and sex-matched wild type mouse hearts (Figure 2J).

Developmental downregulation of miR-184 expression in the heart

In situ hybridization detected expression of miR-184 in E16.5, P3, and P90 hearts (Figure 3A). MiR-184 was abundantly expressed in the embryonic hearts and exhibited progressive downregulation from embryonic to P90 adult hearts (Figure 3A). To further quantify miR-184 levels during cardiac myocyte differentiation, its levels were quantified in E16.5, P3, P21 and P90 hearts. As shown in Figure 3B, miR-184 levels were about 100-fold higher in E16.5 hearts than in P90 adult hearts and were progressively reduced in E16.5, P3 P21 and P90 hearts (Figure 3B).

Differential downregulation of miR-184 in cardiac myocytes isolated from the Nkx2.5-Cre:Pkp2^{shRNA} mice

To further corroborate differential expression of miR-184 in AC, cardiac myocytes were isolated from P3, P21 and P90 wild type and *Nkx2.5-Cre:Pkp2*^{shRNA} mice. Levels of *Pkp2* mRNA were reduced by 40 to 50% in cardiac myocytes isolated from the heart of *Nkx2.5-Cre:Pkp2*^{shRNA} mice, as compared to wild type mice at all three stages of development (Online Figure 1A). MiR-184 levels were the highest in the neonatal (P3) cardiac myocytes, intermediary in P21 cardiac myocytes (4-fold reduction from P3 to P21), and the lowest in P90 cardiac myocytes (10-fold reduction) (Online Figure 1B). Developmental downregulation of miR-184 expression in cardiac myocytes was differential between the wild type and the *Nkx2.5-Cre:Pkp2*^{shRNA} mice, as miR-184 levels were consistently lower by approximately 40% in cardiac myocytes isolated from the *Nkx2.5-Cre:Pkp2*^{shRNA} mice in all three development ages, as compared to the corresponding levels in the wild type mice (Online Figure 1B).

Expression of miR-184, PKP2, and NKX2-5 in cardiac MPCs

Given that miR-184 was expressed at higher levels in immature cardiac cells and was downregulated in mature myocytes, we quantified miR-184 levels in cardiac MPCs, identified as Lin^{neg};PDGFRA^{pos}:CD44^{pos} cells. Consistent with the higher expression levels of miR-184 in the embryonic heart and immature myocytes, miR-184 levels were higher (249.4±57.17 –fold) in cardiac MPCs, as compared to isolated P90 cardiac myocytes (Figure 3C).

To determine whether PKP2 is also expressed in cardiac MPCs, in addition to cardiac myocytes, MPCs were isolated from the hearts of wild type mice and stained for the

expression of PKP2. Likewise, isolated cardiac MPCs were also stained for the expression of NKX2-5, which drives expression of an shRNA against *Pkp2* transcript in the *Nkx2.5*-Cre:*Pkp2*^{shRNA} mice. Consistent with our recent data on the expression of desmosome proteins in non-myocyte cells in the heart [36], PKP2 as well as NKX2-5 were expressed in isolated cardiac MPCs (Figure 3D). Quantitatively 33.45±17.13% of cardiac MPCs express PKP2, 30.0 ±5.9% express NKX2-5 and only 21.2±6.3% of MPCs stained for both PKP2 and NKX2.5 (Figure 3E).

Given heterogeneous expression of PKP2 in cardiac MPCs, to further define the role of miR-184 in differentiation of cardiac MPCs to adipocytes, *Pkp2* transcript was targeted in isolated cardiac MPCs, using 2 sets of lentiviruses expressing distinct *Pkp2*-specific shRNAs (Figure 3F). Knock down of *Pkp2* with both shRNAs (85±6.4% with shRNA1 and 61.2±9.5% with shRNA2) was associated with reduced expression levels of miR-184 (46±26% and 33.6±27%, respectively) in cardiac MPCs (Figures 3F, G).

Regulation of expression of miR-184 by the E2F1 pathway

To gain insights into the mechanisms responsible for downregulation of miR-184 in the AC models, we analyzed differentially expressed transcripts in the HL-1$^{Pkp2\text{-}shRNA}$ cells by RNA-Seq [15]. Pathway analysis led to identification of multiple perturbed signaling pathways including the Hippo, canonical Wnt and integrin signaling pathways in the HL-1$^{Pkp2\text{-}shRNA}$ cells [15]. Notable among the target genes was *Ccnd1*, whose expression was consistently reduced by more than 10-fold. CCND1 is a regulatory subunit of cyclin-dependent kinases 4 and 6, which target retinoblastoma protein (RB1) for inactivation by phosphorylation, and hence, removal of the inhibitory effects of RB1 on E2F transcription factors (Online Figure II). Thus, a dramatic reduction in *Ccnd1* expression is expected to lead to activation of RB1 and suppression of the E2F1 pathway. In accord with the above, Gene Set Enrichment Analysis showed significant downregulation of the E2F1 targets (Figure 4A). Likewise, E2F1 target genes were significantly downregulated in the HL-1$^{Pkp2\text{-}shRNA}$ cells (Figure 4B). Consistent with suppressed E2F1 transcriptional activity and reduced CCND1 levels, proliferation rate of HL-1$^{Pkp2\text{-}shRNA}$ cells was considerably slower, as compared to wild type HL-1 cells (Figure 4C).[15] To determine whether E2F1 directly regulated expression of miR-184, its binding to the promoter region of miR-184 was analyzed by ChIP assay. Genomic DNA was precipitated with an anti E2F1 antibody and miR-184 promoter region was amplified by PCR. The finding indicated binding of E2F1 transcription factor to the promoter region of miR-184 (Figure 4D, E). To further support the role of E2F1 in transcriptional regulation of miR-184, expression of RB1, an inhibitor of E2F1, was suppressed by siRNA targeting. Suppression of *Rb1* expression (3.7±0.6) led to a ~ 2-fold increase in miR-184 transcript levels (Figure 4F). In a complementary set of studies, HL-1$^{Pkp2\text{-}shRNA}$ cells were transduced with recombinant adenoviruses expressing CCND1, which activates the E2F1 transcription factor pathway. Over-expression of CCND1 in HL-1$^{Pkp2\text{-}shRNA}$ cells led to a 1.7-fold increase in the miR-184 transcript levels (Figure 4G).

Effects of the Hippo pathway on miR-184 levels

To determine whether activation of the Hippo pathway, observed in AC [15], was responsible for suppressed miR-184 levels, the Hippo pathway kinases LATS1/2 were inactivated, in

order to activate gene expression through YAP-TEAD transcription factors, upon treatment of the cells with 1 M of LPA for 1, 2, and 4h. Treatment with LPA, increased nuclear localization of YAP (Online Figure IIIA, B), TEAD transcriptional activity; as detected by a luciferase assay (Online Figure IIIC), and YAP-TEAD target transcript levels (Online Figure IIID). However, despite increased YAP-TEAD transcriptional activity, levels of miR-184 were unchanged (Online Figure IIIE-G).

In a complementary set of studies, the YAP-TEAD complex was transcriptionally inactivated upon transduction of the HL-1 cells with Lenti: *Yap*^{shRNA} construct, which expresses an shRNA against *Yap* mRNA. YAP protein levels were reduced by 41% (Online Figure III-H), as were the transcript levels of its down stream targets *Ctgf* and *Cyr61* (Online Figure III-I). However, despite knock down of the YAP-TEAD transcriptional activity, levels of miR-184 levels remained unchanged as compared to control non-transduced cells or cells transduced with a control shRNA (Online Figure III-J).

Effects of the canonical Wnt signaling pathway on miR-184 levels

To ascertain whether suppressed canonical Wnt signaling was responsible for reduced miR-184 levels, the canonical Wnt signaling was activated by treating the HL-1 and HL-1$^{PKP2\text{-}shRNA}$ cells with 40, 80, and 120 ng/ml of the purified Wnt-3A protein. Activation of the canonical Wnt signaling led to a dose–dependent increase in the TCF7L2 luciferase activity (Online Figure IVA) and levels of selected canonical Wnt target transcripts *Ccnd1* and *Axin2* by 2 to 5 -fold (Online Figure IVB). However, activation of the canonical Wnt signaling had no effect on miR-184 levels in the HL-1 cells (Online Figure IVC). Likewise, treatment with Wnt-3A increased TFC7L2 luciferase activity (Figure IVD) and levels of the established canonical Wnt targets in HL-1$^{Pkp2\text{-}shRNA}$ cells (Online Figure IVE). MiR-184 levels were increased only modestly (1.6-fold, N=5, p=0.06, Online Figure IVF). In a complementary set of studies, the canonical Wnt signaling was inactivated upon transduction of the cells with a Lenti: *Tcf7l2*^{shRNA} construct expressing an shRNA targeted to *Tcf7l2* transcription factor. Lentiviral transduction effectively reduced TCF7L2 protein levels by ~ 50% in the HL-1 cells (Online Figure IVG) and the transcripts levels of canonical Wnt targets *Ccnd1* and *Axin2* (Online Figure IVH). However, suppression of the canonical Wnt signaling had no discernible effect on the expression levels of miR-184 (Online Figure IV-I).

Effects of miR-184 on Hippo and canonical Wnt signaling

To determine whether miR-184 was involved in suppression of gene expression through the YAP-TEAD and CTNNB1-TCF7L2 transcription factors, HL-1 cells were transduced with Lenti-miR-184^{shRNA} or Lenti-pre-miR-184 constructs to knock down or over-express miR-184 in HL-1 cells, respectively (Online VA-G). Transduction efficiency was determined by flow cytometric analysis of cells expressing the reporter protein GFP (Online Figure VD, E). Knock down and over-expression of miR-184 were verified by quantification of miR-184 transcript levels (Online Figure VF, G). Neither suppression nor increased expression of miR-184 had any effects on expression levels of selected targets of the Hippo (TEAD-YAP) and canonical Wnt (CTNNB1-TCF7L2) signaling pathways (Online Figure VH, I).

Epigenetic silencing of the miR-184 locus by hypermethylation

Because activation of E2F1 only partially rescued miR-184 levels and given that modulation of the Hippo and canonical Wnt had no significant effect on miR-184 expression, we surmised that additional mechanism(s) might contribute to suppressed miR-184 levels in the HL-1$^{Pkp2\text{-}shRNA}$ cells. The E2F/RB1 complex is known to recruit DNA methyltransferases (DNMTs) to gene promoters [43]. Given that miR-184 resides in an imprinted locus, regulated by methyl-CpG binding domain proteins MBD1 and MeCP2, we determined methylation state of miR-184 5' genomic region. A total of 15 CpG rich regions were identified in the upstream regulatory region of miR-184 locus, which were screened for methylation (Figure 5A). Bisulfite conversion, cloning, and sequencing showed the CpG sites were predominantly unmethylated in the control HL-1 cells (Figure 5B). In contrast, the vast majority of the CpG sites were hypermethylated in HL-1$^{Pkp2\text{-}shRNA}$ cells (Figure 5C). On average, HL-1 cells showed 23% CpG methylation in miR-184 regulatory region, in contrast to 90% CpG methylation in the HL-1^{Pkp2shRNA} cells (Figure 5D). All the 15 identified CpGs showed greater hypermethylation in the HL-1^{Pkp2shRNA} cells (Online Table IV).

To further validate the role of CpG methylation in miR-184 expression, control HL-1 and HL-1$^{PKP2\text{-}shRNA}$ cells were treated with the nucleotide analogue, 5-aza-2′-deoxycytidine (5-azaD) for 5 days. Treatment with 5-aza-D increased miR-184 levels in the control HL-1 and HL-1$^{PKP2\text{-}shRNA}$ cells. However, the magnitude of induction was greater in the HL-1$^{PKP2\text{-}shRNA,}$ as compared to control HL-1 cells (2.4±0.2 -fold vs. 1.8±0.1 -fold, respectively, N=3, p=0.004, Figure 5E). Nevertheless, despite increased expression of miR-184 upon treatment with 5-azaD, its level in the HL-1$^{PKP2\text{-}shRNA}$ cells remained reduced as compared to the controls HL-1 cells, indicating a partial rescue.

To delineate the mechanism(s) responsible for hypermethylation of the CpG site in the 5-genomic region of miR-184, we analyzed recruitment of DNMT1 to the promoter region of miR-184 by ChIP assay. As shown in Figure 5F, genomic fragment of miR-184 was precipitated with an anti DNMT1 antibody and the magnitude of the precipitated DNA was greater in HL-1$^{PKP2\text{-}shRNA}$ cells as compared to wild type HL-1 cells (Figure 5G, 2.1±0.8 -fold, p=0.0.17). To further substantiate the role of DNMT1 in suppression of miR-184 levels, DNMT1 was targeted by recombinant lenti-viruses expressing an shRNA against *Dnmt1* transcript. Knock down of *Dnmt1* by shRNA led to increased miR-184 levels (Figure 5H and I, 1.6±0.2 -fold, N=4, p=0.03).

Integrated miRNA-mRNA analysis

To delineate biological significance of downregulation of miR-184 in AC models, and considering pleiotropic targeting of multiple mRNAs by a single miRNA, we performed a pairwise analysis of miR-184 and the differentially expressed mRNA targets in the HL-1$^{PKP2\text{-}shRNA}$ cells (Figure 6A, B). Only mRNA transcripts that met the target selection criteria were curated. Pairing of miR-184 and its known and predicted target mRNAs led to identification of 145 genes, whose expression levels were increased by 1.2-fold and 40 genes whose expression levels were increased by at least 2-fold (Figure 6C). Gene ontology over-representation analysis (Figure 6D) identified mRNA clusters that were enriched for cellular death and survival (51 transcripts), growth and differentiation (51 transcripts), and cellular

development (11 transcripts). MiR-184 target genes involved specifically in cellular differentiation were further curated and their sub-cellular localization map is depicted in Figure 6E.

MiR-184 and transcriptional switch to adipogenesis

Pathway analysis of paired miR-184 and its mRNA targets also identified networks of genes involved in lipid biosynthesis (Figure 7A). Analysis of target transcripts in the networks showed upregulation of more than a dozen genes involved in lipid biosynthesis in the HL-1$^{PKP2\text{-}shRNA}$ as compared to the control cells (Figure 7B). *Agpat1*, *Agpat3*, *Ncoa3*, *Ppargc1b*, *Dgat1*, *Dgat2*, and *Lpl*, regulators of lipid biosynthesis, were upregulated by 2- to 4-fold (Figure 7B). Upregulation of a selected number of genes in the lipid biosynthesis networks was also validated by qPCR (Figure 7C). Moreover, expression of the adipogenic transcription factor PPARG was increased and fat droplets were accumulated in the HL-1$^{Pkp2\text{-}shRNA}$ cells (Figures 7D-G). Knockdown of *Pkp2* in MPCs also led to enhanced adipogenesis, as evidenced by increased number of cells expressing CEBPA (Figure 7H and J) and accumulating fat droplets (Figure 7I and K).

To determine whether the adipogenic genes identified in the pairwise miR-184-mRNA analysis were directly targeted by miR-184, the 3' untranslated regions (3'UTR) of the candidate genes were analyzed for the presence of miR-184 seed sequence. The 3' UTR of *Agpat3, Ncoa3, Ppargc1b* and *Dgat1* are conserved in mouse and human and were aligned with miR-184 seed sequence (Online Figure VI).

To validate the findings experimentally, HL-1 cells were transduced with recombinant lentiviruses expressing either an shRNA against miR-184 (Lenti:*miR-184*^{shRNA}) or *pre-miR-184*, to suppress or increase miR-184 levels, respectively (Online Figure V). Suppression and over-expression of miR-184 was confirmed by qPCR (Figure 7L). Knock down of miR-184 was associated with increased transcript levels of *Agpat1* and *Agpat3* (Figure 7M). In contrast, over-expression of miR-184 was associated with a modest but a significant decrease in the transcript levels of *Agpat1* and *Agpat 3* (Figure 7M). However, knock down and over-expression of miR-184 did not affect *Ncoa3* and *Ppargc1b* transcript levels, suggesting that mRNAs of these two genes were not directly targeted for degradation by miR-184 (Figure 7M).

Effects of miR-184 on adipogenesis

To further substantiate the causal role of miR-184 in adipogenic differentiation, expression of adipogenic markers and accumulation of fat droplets were analyzed after suppression and over-expression of miR-184 in HL-1 cells and cardiac MPCs (Figure 8). Knock down of miR-184 (Figure 8A) increased transcript levels of *Agpat1* (24% increase, N=3, p=0.001), *Agpat3* (20% increase, N=3, p=0.007), *Pparg* (2.1±0.6 -fold, N=4, p=0.002), and *Fabp4,* a downstream target of PPARG (4.1±3.1 -fold, N=4, p=0.02) in HL-1 cells (Figure 8B). Knock down of miR-184 in cardiac MPCs (Figure 8C) also had similar effects on the transcript levels of the above adipogenic genes (Figure 8D). In contrast, over-expression of miR-184 had the opposite effects in both HL-1 cells and cardiac MPCs (Figure 8C and D). Immunofluorescence staining of HL-1 cells and cardiac MPCs for the expression of

adipogenic transcription factors PPARG and CEBPA showed increased and decreased levels of the adipogenic transcription factors upon knock down and over-expression of miR-184, respectively (Figure 8E-H). Finally, suppression of expression of miR-184 was associated with increased accumulation of fat droplets in HL-1 cells and in cardiac MPCs, while over-expression had the opposite effects (Figure 8I-L).

Rescue of adipogenesis upon over-expression of miR-184 in PKP2-deficient HL-1 cells

To rescue enhanced adipogenesis in the HL-1$^{PKP2\text{-}shRNA}$ cells, cells were transduced with the Lenti:*pre-miR-184* construct to over-express miR-184 (Figure 9A). Expression of miR-184 was evaluated by qPCR, FACS sorting of GFP+ cells, and quantification of miR-184 target transcript levels (Figure 9B-D). As shown in Figure 9A, overexpression of miR-184 was associated with a significant reduction in the transcript levels of *Pparg* (25±10%, N=5, p=0.008), *Fabp4* (25±7%, N=5, p=0.02), *Agpat1* (28±9%, N=5, p=0.0002) and *Agpat3* (25±7%, N=5, p=0.0005). Likewise, the number of cells that contained fat droplets was decreased upon over-expression of miR-184, as compared to non-transduced HL-1$^{PKP2\text{-}shRNA}$ cells (25±3% vs. 17.6±4%, respectively, N=3, 200 cells per group per experiment, p=0.01, Figure 9E, F). Moreover, over-expression of miR-184 reduced the number of PPARG expressing HL-1$^{Pkp2\text{-}shRNA}$ cells (18.43±2.5 vs 14.37±1.5%, N=5, p=0.045, Figure 9G, H). Overexpression of miR-184 only attenuated and did not completely rescue enhanced adipogenesis in the PKP2-deficient cells, as the number of cells with fat droplet remained greater in the transduced HL-1$^{PKP2\text{-}shRNA}$ cells as opposed to the non-transduced control HL-1 levels (25±3 % vs. 5.4±1.0%, respectively, N=5, p=0.001).

DISCUSSION

The findings of the present study implicate miR-184, whose expression is progressively reduced in cardiac myocytes during cardiac development, in the pathogenesis of enhanced adipogenesis in PKP2-deficient cells. Levels of miR-184 were markedly reduced in in vitro and in vivo models including a new *Pkp2*-knock down mouse model of AC. The mechanisms responsible for downregulation of miR-184 levels included suppression of the E2F1 pathway, which regulates miR-184 expression upon binding of E2F1 to its 5' genomic region (Online Figure II). In addition, recruitment of DNMT1 leads to epigenetic silencing of the miR-184 locus upon hyper-methylation of the CpG rich regions. Downregulation of miR-184 levels was associated with upregulation of its target genes involved in cell death, growth, proliferation, and differentiation. Notable among the perturbed pathways was upregulation of genes involved in lipid synthesis and enhanced adipogenesis. Over-expression and knock down of miR-184 suppressed and enhanced adipogenesis, respectively, in HL-1 cells and cardiac MPCs. These findings collectively implicate miR-184 in the pathogenesis of excess adipogenesis in PKP2-deficient cells.

MicroRNA profiling and the mechanistic studies were performed in the HL-1 cells and selected findings, including the effects of miR-184 on adipogenesis, were confirmed in cardiac MPCs. The approach was in keeping with the higher expression levels of miR-184 in cardiac MPCs and murine embryonic hearts, as opposed to mature cardiac myocytes, which expressed miR-184 at low levels. Moreover, adult cardiac myocytes are terminally

differentiates cells with limited, if any, capacity for fate switch. In contrast, MPCs have the potential to differentiate to different lineages and been identified as a cell source of adipocytes in AC [36, 44]. Nevertheless, despite demonstration of the role of MiR-184 in regulating cell fate in two different cell types, the findings merit testing in in vivo models, in order to determine contributions of miR-184 to adipogenesis in AC.

The study by no means is designed to identify all differentially expressed miRNAs or mRNAs in the PKP2-deficient cells or mouse models of AC. The small sample size in the miRNA screening study is expected to lead to under-detection of differentially expressed miRNAs as well as mRNAs (type II statistical error). Nevertheless, differential expressions of the candidate miRNAs, including miR-184, and mRNAs of interest were verified by qPCR in multiple sets of independent experiments. Differentially expressed miRs and mRNA were detected upon comparing the PKP2-competent and PKP2-deficient cells but not PKP2-deficient HL-1 cells and cells transfected with an NT-shRNA vector. The latter had no discernible effects on the transcript levels of selected miRs and mRNAs.

The current gene transfer and genetic engineering methods do not afford the opportunity to manipulate expression of miR-184 in the subset of $CD44^{pos}$/$PDGFRA^{pos}$/$NKX2\text{-}5^{pos}$ cardiac MPCs specifically and efficiently in order to assess in vivo phenotypic effects of manipulation of miR-184 levels. Moreover, it is also not feasible to isolate and further characterize the $CD44^{pos}$/$PDGFRA^{pos}$/$NKX2\text{-}5^{pos}$ cells in vitro. Consequently, the relevance of the mechanistic studies, performed in cell culture systems to in vivo models and human AC remains to be determined. Additional studies in in vivo models would be needed to delineate the role of miR-184 in the pathogenesis of AC.

MiR-184, an evolutionary conserved intergenic single-copy miR, was the most differentially expressed miRNA in two independent lines of HL-$1^{Pkp2\text{-}shRNA}$ cells. PKP2 levels were reduced similarly between the two lines. Hence, a dose-dependent effect of PKP2 suppression on miR-184 levels could not be determined. The initial studies were performed in the HL-1 cells and the findings provided the impetus for generation and characterization of the *Pkp2*-deficient mice. *Ab initio* studies in cardiac MPCs are considered more pertinent and aligned with the working hypothesis. MicroRNA-184 was also downregulated in cardiac myocytes isolated from the AC models and in two independent mouse models of AC, including the new *Nkx2.5*-Cre:$Pkp2^{shRNA}$ and the established *Jup* transgenic ($Myh6{:}Jup^{Tr}$) mouse models [37]. Whether mechanisms similar to those observed in the PKP2-deficiency models are also responsible for downregulation of miR-184 in the heart in the $Myh6{:}Jup^{Tr}$ mice remain to be determined. Several other miRNAs were also dysregulated in the HL-$1^{Pkp2\text{-}shRNA}$ cells. However, among the most dysregulated miRNAs, expression of miR-184 was consistently suppressed in the HL-1 cells and mouse models. The magnitude of reduction was greater in the HL-$1^{Pkp2\text{-}shRNA}$ cells by about 16-fold as compared to ~ 2-fold reduction in the heart of the genetic mouse models. Milder reductions in the heart of transgenic models likely reflect cellular heterogeneity of the heart, expression of miR-184 only in a subset of cardiac cells, and downregulation of miR-184 levels in the adult heart. Knock down of the *Pkp2* gene under transcriptional regulation of the *Nkx2.5* locus predominantly deletes *Pkp2* in cardiac myocytes. NKX2-5 and PKP2, despite being predominantly expressed in the cardiac myocyte lineage, are also expressed in non-myocyte

cells in the heart, including a subset of cardiac MPCs, as shown in the present and previous studies [36]. Such cellular heterogeneity in the expression of the key molecules relevant to the pathogenesis of AC may account for the discrepancy in the magnitude of reductions of miR-184 levels in vitro and in vivo models. Nevertheless, the findings are in agreement with the notion that only a subset of cardiac progenitor cells differentiates to fibro-adipocytes in AC [2, 36, 45].

In view of a more pronounced reduction of miR-184 levels in the HL-1$^{Pkp2\text{-}shRNA}$ cells, phenotypic effects and the mechanistic studies were performed primarily in the HL-1 cells and subsequently in cardiac MPCs, surmising that the in vitro studies would provide a more sensitive platform for delineating the underpinning mechanisms than studies performed on the whole heart. These data are in keeping with our hypothesis that it is a subset of cardiac progenitor cells and not mature cardiac myocytes that differentiate to adipocytes in AC [2, 37, 38, 45]. To strengthen the evidence for the observed effects, the biological effects of miR-184 were analyzed by complementary methods of over-expression and knock down approaches in two independent cell types. Phenotypic consequences, including adipogenesis were detected by independent complementary methods, such as qPCR of the genes involved in lipid biosynthesis, immunofluorescence staining for adipogenic transcription factors, and Oil Red O staining of fat droplets. Collectively, the findings provide strong evidence for the role of miR-184 in the pathogenesis of AC.

In accord with targeting of multiple mRNAs by a single miR, and hence, phenotypic pleiotropy of each miRNA, miR-184 is also implicated in various biological processes, notable among them cell lineage specification [46-48]. Suppression of miR-184 has been associated with reduced cellular proliferation, clonal expansion and differentiation of several progenitor and precursor cells [46-48]. Consistent with the role of miR-184 in cell fate determination, suppressed expression of miR-184, whether upon shRNA-mediated targeting or indirectly upon knock down of PKP2, was associated with a transcriptional switch to adipogenesis and enhanced fat accumulation. At the molecular level, genes encoding AGPAT1 and AGPAT3, which convert lysophosphatidic acid (LPA) into phosphatidic acid (PA) in lipid biosynthetic pathways, were identified as novel targets of miR-184 [49]. In accord with these findings, over-expression of AGPAT1 is shown to increase fatty acid uptake, triacylglycerol production, and accumulation of fat droplets in the 3T3-L1 and C2C12 cells [50]. Likewise, *Ncoa3* and *Ppargc1b,* which have prominent roles in adipogenic differentiation, along with several other adipogenic genes were up regulated upon knock down of PKP2. Transcriptionally, miR-184 targets *Numbl*, *Sox17*, *Ncor2*, and *Akt2* are known to regulate cellular differentiation [47, 51]. In view of multiplicity of miRNA targets, the phenotype consequent to down-regulation of miR-184 in HL-1$^{Pkp2\text{-}shRNA}$ cells or cardiac MPCs is the collective effects of changes in the expression levels of multiple targets and not a single target. The pleiotropic of effects hinders from manipulation a single miR-184 target as a means of phenotypic rescue. Consequently, the rescue experiments were performed upon over-expression of miR-184 in the HL-1$^{Pkp2\text{-}shRNA}$ cells, which exhibit suppressed miR-184 levels. Collectively, the new findings along with the existing data support a role of miR-184 as a homeostatic balancer of proliferation and differentiation.

The effect size of miR-184 on the levels of its target transcripts were relatively modest, a finding that is consistent with the established role of miRNAs as “nudgers and tweakers of genome management” [21]. These subtle changes in gene expression and phenotype are inherent to miRNA regulatory networks that are not only dependent on the changes in miRNA concentration, but also stoichiometric amounts of its target. Furthermore, miRs in general behave as a temporal agent to control targets or signaling networks by setting a threshold of expression, thus allowing or amplifying a signal in cohort with other transcription factors. Accordingly, in a complex phenotype such as AC, the phenotype is the consequence of a myriad of molecular changes that occur, including changes in the levels of multiple miRNA, as observed in the present study, each contributing to the phenotype and none alone is a sole determinant.

MiR-184 is located in an imprinted locus on mouse chromosome 9, and it is repressed upon methylation of the CpG rich sequences at its promoter region [47]. In accord with the epigenetic silencing of the miR-184 locus, the upstream regulatory sites of miR-184 were hypermethylated in in the HL-1$^{Pkp2\text{-}shRNA}$ cells. DNA methylation-dependent repression of miR-184 transcription occurs by binding of methyl-CpG binding protein 1 (MBD1) and methyl-CpG protein binding (MeCP2) to the methylated regions [47, 52]. Treatment with 5-azaD and suppression of DNMT1, as well as activation of the E2F1 transcription pathway induced expression of miR-184 levels in HL-1 cells. Nevertheless, the magnitude of induction was insufficient to normalize the miR-184 levels in the HL-1$^{Pkp2\text{-}shRNA}$ cells. Failure to completely rescue suppressed miR-184 levels might reflect irreversible epigenetic silencing of this locus in the HL-1$^{Pkp2\text{-}shRNA}$ cells. Moreover, several other mechanisms that were delineated, particularly cell contact regulators, such as integrins, might contribute to down-regulation of the miR-184 levels in the PKP2-deficient HL-1 cells, which were not studied. The mechanism(s) by which PKP2 impacts methylation of the miR-184 locus is likely related to recruitment of DNMT1 by the RB1/E2F1 complex to the 5’ genomic region of miR-184 (Online Figure II). The two delineated mechanisms, namely suppression of E2F1 and hypermethylation of 5’ genomic region of miR-184 offer a unifying mechanism regulated by CCND1, which is markedly suppressed in the AC models [15]. CCND1 is a regulator of CDK4/6, which target RB1 for inactivation upon phosphorylation and hence, gene expression through E2F1 transcription factor (Online Figure II). Consequently, reduced CCND1 levels and activation of RB1 might enhance recruitment of DNMT1 to the genomic regions [43]. Finally, given that PKP2 is known to localize to the nucleus in addition to the IDs [53, 54], it is intriguing to postulate a role of the PKP2 in recruitment and assembly of DNA Methyltransferases, directly or through interactions with other proteins in the promoter complex. As a whole, the findings suggest a primary role for increased CpG methylation, but also the involvement of multiple mechanisms including suppression of E2F1 pathway in downregulation of miR-184 levels in the HL-1$^{Pkp2\text{-}shRNA}$ cells.

Activation of the Hippo pathway and reduced gene expression through its downstream effectors YAP-TEAD and the canonical Wnt signaling, which are impaired in the HL-1$^{Pkp2\text{-}shRNA}$ cells [15, 16], did not significantly influence miR-184 levels. Likewise, over-expression or knock down of miR-184 did not affect transcriptional activities of these pathways. In contrast to a recent report indicating that miR-184 suppresses the canonical Wnt signaling in retina [55], over-expression of miR-184 had no discernible effects on the

transcript levels of selected canonical Wnt signaling targets in HL-1 cells. By-and-large, suppressed expression levels of miR-184 were independent of the Hippo and canonical Wnt signaling pathway transcriptional activities in HL-1 cells.

In conclusion, the findings of the present study show pathogenic down regulation of miR-184 in PKP2-deficient cells and mouse models of AC. The responsible mechanisms include suppression of the E2F1 transcription factor pathway and epigenetic silencing of miR-184 genomic locus upon CpG methylation. MiR-184 regulates adipogenesis in HL-1 cells and a subset of cardiac MPCs that express intercalated disc protein PKP2. The findings illustrate a pathogenic role for miR-184 in cellular proliferation and enhanced adipogenesis PKP2-deficiency.

Supplementary Material

Refer to Web version on PubMed Central for supplementary material.

Acknowledgments

SOURCES OF FUNDING

This work was supported in part by grants from NIH, National Heart, Lung and Blood Institute (NHLBI, R01 HL088498, 1R01HL132401, and R34 HL105563), Leducq Foundation (14 CVD 03), Roderick MacDonald Foundation (13RDM005), TexGen Fund from Greater Houston Community Foundation, Texas Heart Institute Foundation, and George and Mary Josephine Hamman Foundation. Dr. Xiaofan Chen was supported as a PhD student for his work at the Center for Cardiovascular Genetics, the University of Texas Health Science Center-Houston, for one year by a grant from China Scholarship Council, sponsored by Dr. Yiming Ni at the Zhejiang University, China.

Nonstandard Abbreviations and Acronyms

5-aza-D	5-Aza-2′-deoxycytidine
AC	Arrhythmogenic Cardiomyopathy
Agpat1	Acylglycerolphosphate acyltransferase
Agpat3	Acylglycerolphosphate acyltransferase
copGFP	Copepod Green fluorescent protein
DAPT	N-[N-(3,5-Difluorophenacetyl)-L-alanyl]-S-phenylglycine t-butyl ester
DNMT	DNA methyl transferase
FABP4	Fatty Acid Binding Protein 4
FPKM	Fragments per kilobase of transcript per million fragments mapped
IDs	Intercalated Disc
IPA	Ingenuity pathway Analysis
JUP	Junction Plakoglobin

LPA	lysophosphatidic acid
MBD1	Methyl-CpG Binding Domain Protein 1
MeCP2	Methyl-CpG Binding Protein 2
MPCs	Mesenchymal progentior cells
MiR	MicroRNA
PKP2	Plakophilin-2
PPARG	Peroxisome Proliferator-Activated Receptor Gamma
RB1	Retinoblastoma 1
RNA-Seq	RNA sequencing
ShRNA	Short hairpin RNA
TCF7L2	Transcription Factor 7-Like 2 (T-Cell Specific, HMG-Box)
TEAD	TEA domain family member (SV40 transcriptional enhancer factor)
TLDA	Taqman Low Density Array
YAP	Yes-associated protein

REFERENCES

1. Delmar M, McKenna WJ. The cardiac desmosome and arrhythmogenic cardiomyopathies: From gene to disease. Circulation research. 2010; 107:700–714. [PubMed: 20847325]
2. Lombardi R, Marian AJ. Molecular genetics and pathogenesis of arrhythmogenic right ventricular cardiomyopathy: A disease of cardiac stem cells. Pediatric cardiology. 2011; 32:360–365. [PubMed: 21267716]
3. Basso C, Thiene G, Corrado D, Angelini A, Nava A, Valente M. Arrhythmogenic right ventricular cardiomyopathy. Dysplasia, dystrophy, or myocarditis? Circulation. 1996; 94:983–991. [PubMed: 8790036]
4. Corrado D, Basso C, Thiene G, McKenna WJ, Davies MJ, Fontaliran F, Nava A, Silvestri F, Blomstrom-Lundqvist C, Wlodarska EK, Fontaine G, Camerini F. Spectrum of clinicopathologic manifestations of arrhythmogenic right ventricular cardiomyopathy/dysplasia: A multicenter study. Journal of the American College of Cardiology. 1997; 30:1512–1520. [PubMed: 9362410]
5. McKoy G, Protonotarios N, Crosby A, Tsatsopoulou A, Anastasakis A, Coonar A, Norman M, Baboonian C, Jeffery S, McKenna WJ. Identification of a deletion in plakoglobin in arrhythmogenic right ventricular cardiomyopathy with palmoplantar keratoderma and woolly hair (naxos disease). Lancet. 2000; 355:2119–2124. [PubMed: 10902626]
6. Rampazzo A, Nava A, Malacrida S, Beffagna G, Bauce B, Rossi V, Zimbello R, Simionati B, Basso C, Thiene G, Towbin JA, Danieli GA. Mutation in human desmoplakin domain binding to plakoglobin causes a dominant form of arrhythmogenic right ventricular cardiomyopathy. American journal of human genetics. 2002; 71:1200–1206. [PubMed: 12373648]
7. den Haan AD, Tan BY, Zikusoka MN, Llado LI, Jain R, Daly A, Tichnell C, James C, Amat-Alarcon N, Abraham T, Russell SD, Bluemke DA, Calkins H, Dalal D, Judge DP. Comprehensive desmosome mutation analysis in north americans with arrhythmogenic right ventricular dysplasia/cardiomyopathy. Circulation. Cardiovascular genetics. 2009; 2:428–435. [PubMed: 20031617]

8. Heuser A, Plovie ER, Ellinor PT, Grossmann KS, Shin JT, Wichter T, Basson CT, Lerman BB, Sasse-Klaassen S, Thierfelder L, MacRae CA, Gerull B. Mutant desmocollin-2 causes arrhythmogenic right ventricular cardiomyopathy. American journal of human genetics. 2006; 79:1081–1088. [PubMed: 17186466]

9. Syrris P, Ward D, Evans A, Asimaki A, Gandjbakhch E, Sen-Chowdhry S, McKenna WJ. Arrhythmogenic right ventricular dysplasia/cardiomyopathy associated with mutations in the desmosomal gene desmocollin-2. American journal of human genetics. 2006; 79:978–984. [PubMed: 17033975]

10. Li J, Radice GL. A new perspective on intercalated disc organization: Implications for heart disease. Dermatology research and practice. 2010; 2010:207835. [PubMed: 20585598]

11. Quarta G, Syrris P, Ashworth M, Jenkins S, Zuborne Alapi K, Morgan J, Muir A, Pantazis A, McKenna WJ, Elliott PM. Mutations in the lamin a/c gene mimic arrhythmogenic right ventricular cardiomyopathy. European heart journal. 2012; 33:1128–1136. [PubMed: 22199124]

12. Merner ND, Hodgkinson KA, Haywood AF, Connors S, French VM, Drenckhahn JD, Kupprion C, Ramadanova K, Thierfelder L, McKenna W, Gallagher B, Morris-Larkin L, Bassett AS, Parfrey PS, Young TL. Arrhythmogenic right ventricular cardiomyopathy type 5 is a fully penetrant, lethal arrhythmic disorder caused by a missense mutation in the tmem43 gene. American journal of human genetics. 2008; 82:809–821. [PubMed: 18313022]

13. Gerull B, Heuser A, Wichter T, Paul M, Basson CT, McDermott DA, Lerman BB, Markowitz SM, Ellinor PT, MacRae CA, Peters S, Grossmann KS, Drenckhahn J, Michely B, Sasse-Klaassen S, Birchmeier W, Dietz R, Breithardt G, Schulze-Bahr E, Thierfelder L. Mutations in the desmosomal protein plakophilin-2 are common in arrhythmogenic right ventricular cardiomyopathy. Nature genetics. 2004; 36:1162–1164. [PubMed: 15489853]

14. van Tintelen JP, Entius MM, Bhuiyan ZA, Jongbloed R, Wiesfeld AC, Wilde AA, van der Smagt J, Boven LG, Mannens MM, van Langen IM, Hofstra RM, Otterspoor LC, Doevendans PA, Rodriguez LM, van Gelder IC, Hauer RN. Plakophilin-2 mutations are the major determinant of familial arrhythmogenic right ventricular dysplasia/cardiomyopathy. Circulation. 2006; 113:1650–1658. [PubMed: 16567567]

15. Chen SN, Gurha P, Lombardi R, Ruggiero A, Willerson JT, Marian AJ. The hippo pathway is activated and is a causal mechanism for adipogenesis in arrhythmogenic cardiomyopathy. Circulation research. 2014; 114:454–468. [PubMed: 24276085]

16. Garcia-Gras E, Lombardi R, Giocondo MJ, Willerson JT, Schneider MD, Khoury DS, Marian AJ. Suppression of canonical wnt/beta-catenin signaling by nuclear plakoglobin recapitulates phenotype of arrhythmogenic right ventricular cardiomyopathy. The Journal of clinical investigation. 2006; 116:2012–2021. [PubMed: 16823493]

17. Heallen T, Zhang M, Wang J, Bonilla-Claudio M, Klysik E, Johnson RL, Martin JF. Hippo pathway inhibits wnt signaling to restrain cardiomyocyte proliferation and heart size. Science. 2011; 332:458–461. [PubMed: 21512031]

18. Thum T, Condorelli G. Long noncoding rnas and micrornas in cardiovascular pathophysiology. Circulation research. 2015; 116:751–762. [PubMed: 25677521]

19. Gurha P, Marian AJ. Noncoding rnas in cardiovascular biology and disease. Circulation research. 2013; 113:e115–120. [PubMed: 24311620]

20. Lu TY, Lin B, Li Y, Arora A, Han L, Cui C, Coronnello C, Sheng Y, Benos PV, Yang L. Overexpression of microrna-1 promotes cardiomyocyte commitment from human cardiovascular progenitors via suppressing wnt and fgf signaling pathways. Journal of molecular and cellular cardiology. 2013; 63:146–154. [PubMed: 23939491]

21. Bird A. Genome biology: Not drowning but waving. Cell. 2013; 154:951–952. [PubMed: 23993086]

22. Tian Y, Liu Y, Wang T, Zhou N, Kong J, Chen L, Snitow M, Morley M, Li D, Petrenko N, Zhou S, Lu M, Gao E, Koch WJ, Stewart KM, Morrisey EE. A microrna-hippo pathway that promotes cardiomyocyte proliferation and cardiac regeneration in mice. Science translational medicine. 2015; 7:279ra238.

23. Thompson BJ, Cohen SM. The hippo pathway regulates the bantam microrna to control cell proliferation and apoptosis in drosophila. Cell. 2006; 126:767–774. [PubMed: 16923395]

24. Kim IM, Wang Y, Park KM, Tang Y, Teoh JP, Vinson J, Traynham CJ, Pironti G, Mao L, Su H, Johnson JA, Koch WJ, Rockman HA. Beta-arrestin1-biased beta1-adrenergic receptor signaling regulates microrna processing. Circulation research. 2014; 114:833–844. [PubMed: 24334028]
25. Wang D, Zhang H, Li M, Frid MG, Flockton AR, McKeon BA, Yeager ME, Fini MA, Morrell NW, Pullamsetti SS, Velegala S, Seeger W, McKinsey TA, Sucharov CC, Stenmark KR. Microrna-124 controls the proliferative, migratory, and inflammatory phenotype of pulmonary vascular fibroblasts. Circulation research. 2014; 114:67–78. [PubMed: 24122720]
26. Castaldi A, Zaglia T, Di Mauro V, Carullo P, Viggiani G, Borile G, Di Stefano B, Schiattarella GG, Gualazzi MG, Elia L, Stirparo GG, Colorito ML, Pironti G, Kunderfranco P, Esposito G, Bang ML, Mongillo M, Condorelli G, Catalucci D. Microrna-133 modulates the beta1-adrenergic receptor transduction cascade. Circulation research. 2014; 115:273–283. [PubMed: 24807785]
27. Harada M, Luo X, Murohara T, Yang B, Dobrev D, Nattel S. Microrna regulation and cardiac calcium signaling: Role in cardiac disease and therapeutic potential. Circulation research. 2014; 114:689–705. [PubMed: 24526675]
28. Sun X, He S, Wara AK, Icli B, Shvartz E, Tesmenitsky Y, Belkin N, Li D, Blackwell TS, Sukhova GK, Croce K, Feinberg MW. Systemic delivery of microrna-181b inhibits nuclear factor-kappab activation, vascular inflammation, and atherosclerosis in apolipoprotein e-deficient mice. Circulation research. 2014; 114:32–40. [PubMed: 24084690]
29. Icli B, Wara AK, Moslehi J, Sun X, Plovie E, Cahill M, Marchini JF, Schissler A, Padera RF, Shi J, Cheng HW, Raghuram S, Arany Z, Liao R, Croce K, MacRae C, Feinberg MW. Microrna-26a regulates pathological and physiological angiogenesis by targeting bmp/smad1 signaling. Circulation research. 2013; 113:1231–1241. [PubMed: 24047927]
30. Yang Y, Del Re DP, Nakano N, Sciarretta S, Zhai P, Park J, Sayed D, Shirakabe A, Matsushima S, Park Y, Tian B, Abdellatif M, Sadoshima J. Mir-206 mediates yap-induced cardiac hypertrophy and survival. Circulation research. 2015; 117:891–904. [PubMed: 26333362]
31. Bush EW, van Rooij E. Mir-25 in heart failure. Circulation research. 2014; 115:610–612. [PubMed: 25214573]
32. Kuwabara Y, Horie T, Baba O, Watanabe S, Nishiga M, Usami S, Izuhara M, Nakao T, Nishino T, Otsu K, Kita T, Kimura T, Ono K. Microrna-451 exacerbates lipotoxicity in cardiac myocytes and high-fat diet-induced cardiac hypertrophy in mice through suppression of the lkb1/ampk pathway. Circulation research. 2015; 116:279–288. [PubMed: 25362209]
33. Li CJ, Cheng P, Liang MK, Chen YS, Lu Q, Wang JY, Xia ZY, Zhou HD, Cao X, Xie H, Liao EY, Luo XH. Microrna-188 regulates age-related switch between osteoblast and adipocyte differentiation. The Journal of clinical investigation. 2015; 125:1509–1522. [PubMed: 25751060]
34. Carlson S, Trial J, Soeller C, Entman ML. Cardiac mesenchymal stem cells contribute to scar formation after myocardial infarction. Cardiovascular research. 2011; 91:99–107. [PubMed: 21357194]
35. Cieslik KA, Trial J, Entman ML. Defective myofibroblast formation from mesenchymal stem cells in the aging murine heart rescue by activation of the ampk pathway. Am J Pathol. 2011; 179:1792–1806. [PubMed: 21819956]
36. Lombardi R, Chen SN, Ruggiero A, Gurha P, Czernuszewicz GZ, Willerson JT, Marian AJ. Cardiac fibro-adipocyte progenitors express desmosome proteins and preferentially differentiate to adipocytes upon deletion of the desmoplakin gene. Circulation research. 2016
37. Lombardi R, da Graca Cabreira-Hansen M, Bell A, Fromm RR, Willerson JT, Marian AJ. Nuclear plakoglobin is essential for differentiation of cardiac progenitor cells to adipocytes in arrhythmogenic right ventricular cardiomyopathy. Circulation research. 2011; 109:1342–1353. [PubMed: 22021931]
38. Lombardi R, Dong J, Rodriguez G, Bell A, Leung TK, Schwartz RJ, Willerson JT, Brugada R, Marian AJ. Genetic fate mapping identifies second heart field progenitor cells as a source of adipocytes in arrhythmogenic right ventricular cardiomyopathy. Circulation research. 2009; 104:1076–1084. [PubMed: 19359597]
39. Shukla V, Coumoul X, Wang RH, Kim HS, Deng CX. Rna interference and inhibition of mek-erk signaling prevent abnormal skeletal phenotypes in a mouse model of craniosynostosis. Nature genetics. 2007; 39:1145–1150. [PubMed: 17694057]

40. Shukla V, Coumoul X, Deng CX. Rnai-based conditional gene knockdown in mice using a u6 promoter driven vector. International journal of biological sciences. 2007; 3:91–99. [PubMed: 17304337]
41. Moses KA, DeMayo F, Braun RM, Reecy JL, Schwartz RJ. Embryonic expression of an nkx2-5/cre gene using rosa26 reporter mice. Genesis. 2001; 31:176–180. [PubMed: 11783008]
42. Yaylaoglu MB, Titmus A, Visel A, Alvarez-Bolado G, Thaller C, Eichele G. Comprehensive expression atlas of fibroblast growth factors and their receptors generated by a novel robotic in situ hybridization platform. Dev Dyn. 2005; 234:371–386. [PubMed: 16123981]
43. Robertson KD, Ait-Si-Ali S, Yokochi T, Wade PA, Jones PL, Wolffe AP. Dnmt1 forms a complex with rb, e2f1 and hdac1 and represses transcription from e2f-responsive promoters. Nature genetics. 2000; 25:338–342. [PubMed: 10888886]
44. Sommariva E, Brambilla S, Carbucicchio C, Gambini E, Meraviglia V, Dello Russo A, Farina FM, Casella M, Catto V, Pontone G, Chiesa M, Stadiotti I, Cogliati E, Paolin A, Ouali Alami N, Preziuso C, d'Amati G, Colombo GI, Rossini A, Capogrossi MC, Tondo C, Pompilio G. Cardiac mesenchymal stromal cells are a source of adipocytes in arrhythmogenic cardiomyopathy. European heart journal. 2016; 37:1835–1846. [PubMed: 26590176]
45. Lombardi R, Marian AJ. Arrhythmogenic right ventricular cardiomyopathy is a disease of cardiac stem cells. Current opinion in cardiology. 2010; 25:222–228. [PubMed: 20124997]
46. Shalom-Feuerstein R, Serror L, De La Forest Divonne S, Petit I, Aberdam E, Camargo L, Damour O, Vigouroux C, Solomon A, Gaggioli C, Itskovitz-Eldor J, Ahmad S, Aberdam D. Pluripotent stem cell model reveals essential roles for mir-450b-5p and mir-184 in embryonic corneal lineage specification. Stem cells. 2012; 30:898–909. [PubMed: 22367714]
47. Liu C, Teng ZQ, Santistevan NJ, Szulwach KE, Guo W, Jin P, Zhao X. Epigenetic regulation of mir-184 by mbd1 governs neural stem cell proliferation and differentiation. Cell stem cell. 2010; 6:433–444. [PubMed: 20452318]
48. Iovino N, Pane A, Gaul U. Mir-184 has multiple roles in drosophila female germline development. Developmental cell. 2009; 17:123–133. [PubMed: 19619497]
49. Wilfling F, Wang H, Haas JT, Krahmer N, Gould TJ, Uchida A, Cheng JX, Graham M, Christiano R, Frohlich F, Liu X, Buhman KK, Coleman RA, Bewersdorf J, Farese RV Jr. Walther TC. Triacylglycerol synthesis enzymes mediate lipid droplet growth by relocalizing from the er to lipid droplets. Developmental cell. 2013; 24:384–399. [PubMed: 23415954]
50. Ruan H, Pownall HJ. Overexpression of 1-acyl-glycerol-3-phosphate acyltransferase-alpha enhances lipid storage in cellular models of adipose tissue and skeletal muscle. Diabetes. 2001; 50:233–240. [PubMed: 11272131]
51. Wu GG, Li WH, He WG, Jiang N, Zhang GX, Chen W, Yang HF, Liu QL, Huang YN, Zhang L, Zhang T, Zeng XC. Mir-184 post-transcriptionally regulates sox7 expression and promotes cell proliferation in human hepatocellular carcinoma. PloS one. 2014; 9:e88796. [PubMed: 24558429]
52. Nomura T, Kimura M, Horii T, Morita S, Soejima H, Kudo S, Hatada I. Mecp2-dependent repression of an imprinted mir-184 released by depolarization. Human molecular genetics. 2008; 17:1192–1199. [PubMed: 18203756]
53. Mertens C, Hofmann I, Wang Z, Teichmann M, Sepehri Chong S, Schnolzer M, Franke WW. Nuclear particles containing rna polymerase iii complexes associated with the junctional plaque protein plakophilin 2. Proceedings of the National Academy of Sciences of the United States of America. 2001; 98:7795–7800. [PubMed: 11416169]
54. Chen X, Bonne S, Hatzfeld M, van Roy F, Green KJ. Protein binding and functional characterization of plakophilin 2. Evidence for its diverse roles in desmosomes and beta -catenin signaling. The Journal of biological chemistry. 2002; 277:10512–10522. [PubMed: 11790773]
55. Takahashi Y, Chen Q, Rajala RV, Ma JX. Microrna-184 modulates canonical wnt signaling through the regulation of frizzled-7 expression in the retina with ischemia-induced neovascularization. FEBS letters. 2015; 589:1143–1149. [PubMed: 25796186]

Novelty and Significance

What Is Known?

- Arrhythmogenic cardiomyopathy (AC) is a genetic disease that clinically manifests with ventricular arrhythmias, heart failure, and sudden cardiac death.
- Pathological hallmark of AC is replacement of cardiac myocytes by fibro-adipocytes, particularly in the right ventricle.
- Mutations in genes encoding desmosome (intercalated disk) proteins are identified in approximately half of the families with AC.
- *PKP2*, encoding plakophilin 2, is the most common causal gene for AC.

What New Information Does This Article Contribute?

- Knock down of *Pkp2* in HL-1 cells led to dysregulation of 59 miRNAs.
- MicroRNA-184 was the most down-regulated, while the miR-200 family was the most upregulated microRNAs in the *Pkp2*-knock down HL-1 cells.
- Knock down of *Pkp2* in the mouse heart was also associated with downregulation of miR-184.
- Expression of miR-184 was progressively downregulated during cardiac development, being the highest in early embryonic heart and in cardiac mesenchymal progenitor cells (MPCs) and lowest in adult cardiac myocytes.
- Knock down of PKP2 led to epigenetic silencing of miR-184 through increased recruitment of DNA methyltransferase 1 (DNMT1) and hypermethylation of the CpG sites at its 5’ genomic region, as well as suppression of the E2F1 transcription factor, which regulated miR-184 upon direct binding to the 5’ genomic region.
- Suppression of miR-184 enhanced and its activation attenuated adipogenesis through direct targeting of adipogenic genes in MPCs and HL-1 cells.

MicroRNA-184 is a developmentally regulated miR, whose expression is highest in the embryonic heart and cardiac MPCs and lowest in adult cardiac myocytes. Developmental downregulation of miR-184 is enhanced in PKP2-deficient myocytes. Expression of miR-184 is regulated by the E2F1 transcription factor and CpG hypermethylation at its 5’ genomic region, which are suppressed and enhanced, respectively in PKP2 deficiency. MiR-184 regulates proliferation and adipogenesis in HL-1 cells and cardiac MPCs. The findings suggest a role for miR-184 in the molecular pathogenesis of adipogenesis in

PKP2 deficiency. The findings set the stage for additional studies in in vivo models and humans with AC.

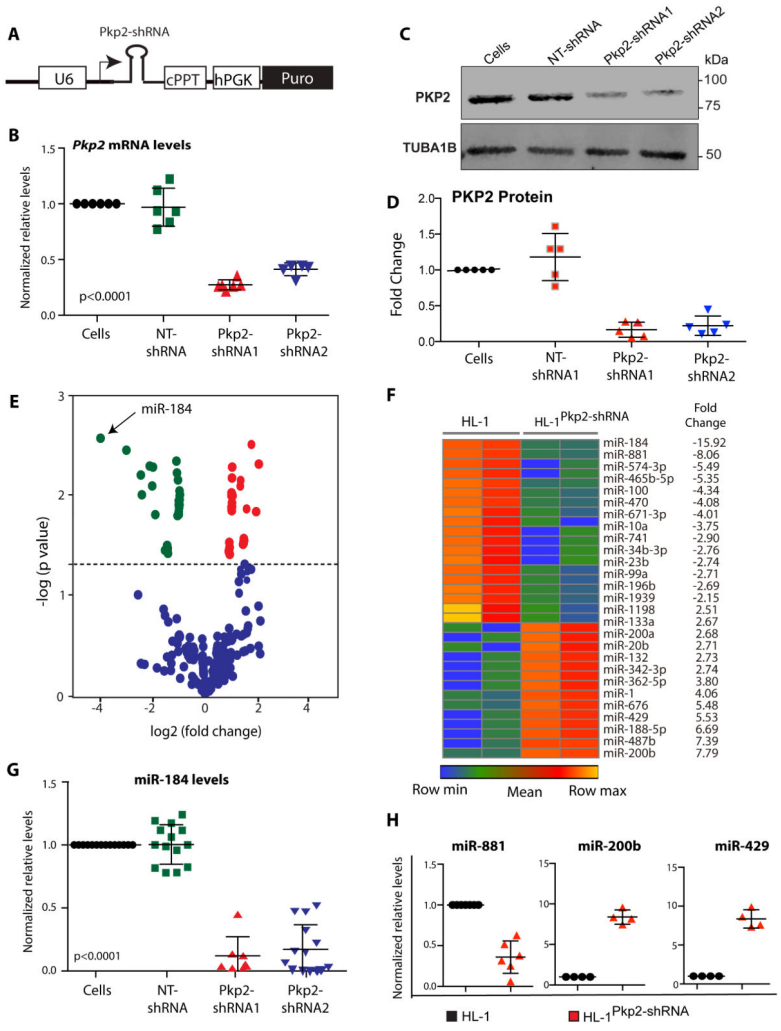

Figure 1. Differentially expressed miRNAs in AC models

A) Schematic representation of shRNA constructs used to knockdown *Pkp2* in the HL-1 (HL-1$^{Pkp2\text{-}shRNA}$) cells. **B)** Quantitative PCR (qPCR) analysis of *Pkp2* mRNA in HL-1 cells expressing two independent shRNAs targeting *Pkp2*. An shRNA with no targeting site in the mammalian genome (NT-shRNA) was used as a control (N=6 per group, p<0.0001 between HL-1 and HL-1$^{Pkp2\text{-}shRNA1}$ or HL-1$^{Pkp2\text{-}shRNA2}$, and p=0.27 between non-transduced HL-1 and HL-1 cells transduced with NT-shRNA by Dunnett's multiple comparisons test). There were no differences in the expression levels of *Pkp2* or selected genes including miRNAs between the NT-shRNA and HL-1 control cells. Therefore, control PKP2-competent HL-1 cells were used as control. **C-D)** Immunoblots (IB) and quantitation graph showing suppression of PKP2 protein in the HL-1$^{Pkp2\text{-}shRNA}$ cells (N=5 per group, p<0.0001 between control cells and cells transduced with shRNA1 and 2 constructs, and p=0.8 for non-transduced cells vs. cells transduced with the NT-shRNA construct). **E)** Volcano Plot of Taqman low-density array data showing log 2-fold change vs. -log p values for all miRNAs in control HL-1 vs. HL-1$^{Pkp2\text{-}shRNA}$ cells. MiR-184, the most differentially expressed miRNA (16-fold downregulation in the HL-1$^{Pkp2\text{-}shRNA}$ cells), is marked. **F)** Heat Map of differentially expressed miRNAs (a 2-fold change cutoff point) between control HL-1 and

HL-1$^{Pkp2\text{-}shRNA}$ cells. **G**) Quantitative PCR data showing suppressed miR-184 expression levels in two independent lines of HL-1$^{Pkp2\text{-}shRNA}$ cells (fshRNA#1 vs. control: 5.86±4.5 -fold, N=7, p<0.0001 and shRNA#2 vs. control, 14.2±9.2 –fold, N=24, p<0.001) **H)** Quantitative PCR confirming reduced levels of miR-881 and increased levels of miR-200b and miR-429 in the HL-1$^{Pkp2\text{-}shRNA}$ cells (N=4-6 per group, and all p values <0.001).

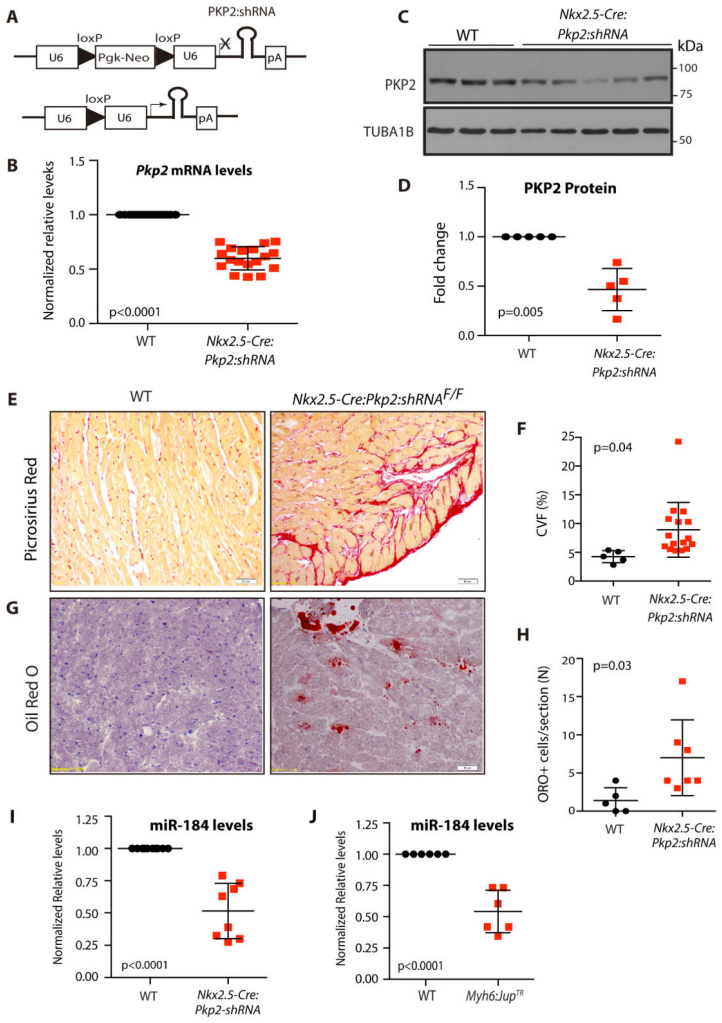

Figure 2. *Pkp2* knock down mouse model of AC

A) Schematic representation of the shRNA construct used to knock down PKP2 conditionally in the mouse heart. **B)** Quantitative PCR (qPCR) data showing efficient *Pkp2* mRNA knock down in the heart in the *Nkx2.5-Cre:Pkp2*^{shRNA} mice as compared to wild type (WT) control (41±10%, N=19, p<0.0001). **C-D)** Immunoblots (IB) and quantitation graph showing suppression of PKP2 protein in the *Nkx2.5-Cre:Pkp2*^{shRNA} mice, as compared to WT control (54±21%, N=5, p=0.005). **E-F)** Thin myocardial sections stained for Picro-Sirius Red showing increased fibrosis in the *Nkx2.5-Cre:Pkp2*^{shRNA} mouse hearts, as compared to WT mice (2.1±1.1 -fold increase, N=5 WT and 16 *Nkx2.5-Cre:Pkp2*^{shRNA} mice). **G-H)** ORO stained thin myocardial sections and quantitative data, respectively, showing increased number of adipocytes in the heart of *Nkx2.5-Cre:Pkp2*^{shRNA} mice (5.1±3.4 -fold, N=5-7 per group). **I and J)** Data showing reduced levels of miR-184 in two independent mouse models of AC. MiR-184 levels were reduced in the PKP2-deficient mice (*Nkx2-5-Cre*$^{Pkp2\text{-}shRNA}$, 2.2±0.97-fold, N=8 per group, p=0.0001), and mice expressing a truncated junction protein plakoglobin (*Myh6:Jup*^{Tr}, 1.99±0.63 -fold, N=6 per group, p<0.0001).

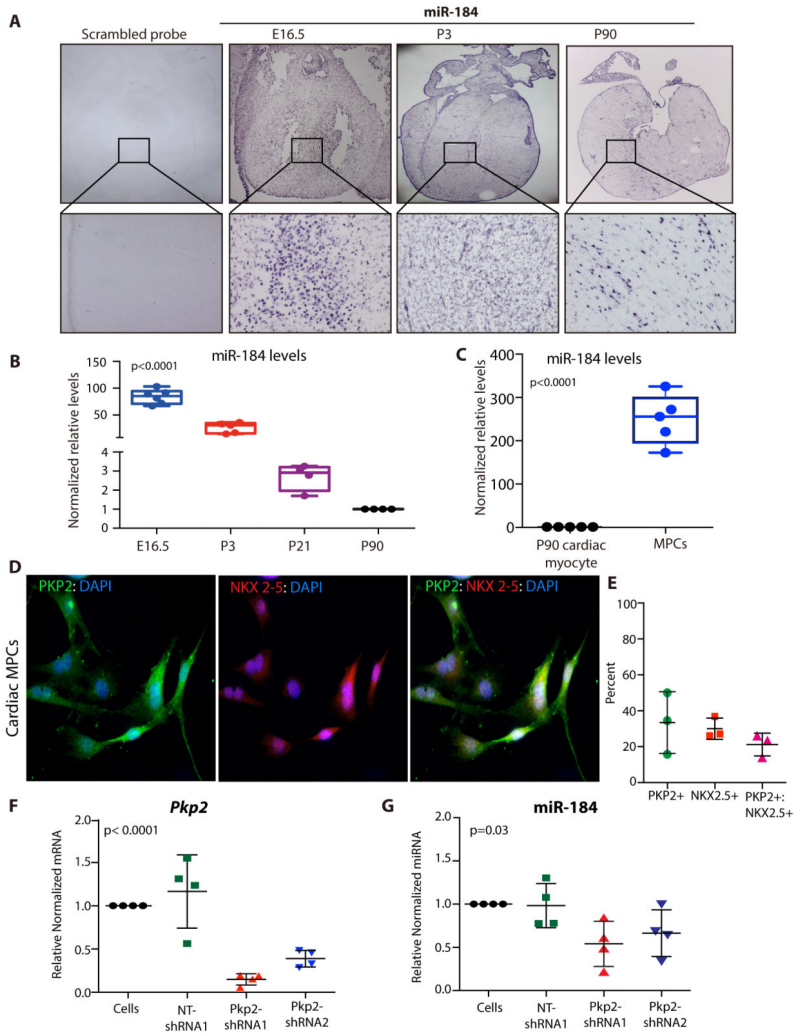

Figure 3. Expression and developmental downregulation of miR-184 in the heart and cardiac MPCs

A) *In situ hybridization* showing expression and progressive reduction in miR-184 levels in E16,6, P3 and P90 hearts. **B**) qPCR data showing progressive downregulation of miR-184 levels in E16.5, P3, P21 and P90 hearts (N=4-6 per group, p<0.001 for all groups compared to E16.5 group, p<0.001 between P90 and E16.5, p=0.002 between P90 and P3, and p=0.1 between P90 and P21). **C**) Expression levels of miR-184 in cardiac MPCs showing 249.4±57.17 -fold higher levels in cardiac MPCs, as compared to adult cardiac myocytes (N=5, p<0.0001). **D**. Expression of PKP2 (green) and NKX2-5 (red) in isolated cardiac MPCs, as detected by immunofluorescence staining. **E**. Quantitative data showing 33.45±17.13% of cardiac MPC expressing PKP2, 30.0±5.9% expressing NKX2-5, and 21.2±6.3% expressing both PKP2, NKX2-5. **F**. Knock down of *Pkp2* in cardiac MPCs using two independent sets of shRNAs. *Pkp2* mRNA levels were reduced by 85±6.4% and 61.2±9.5% with shRNAs 1 and 2, respectively (N=4 per each set, p<0.0001 for each knock down groups compared to non-transduced cells). **G.** Reduced miR-184 transcript levels upon knock down of *Pkp2* in two independent lines in cardiac MPCs (N=4, p=0.03, p=0.02 for pairwise comparisons between the control and Pkp2-shRNA1 groups, and p=0.10 between

control and Pkp2-shRNA1 groups). The control NT-shRNA vector had a backbone identical to that in the viral constructs used to suppress *Pkp2* expression.

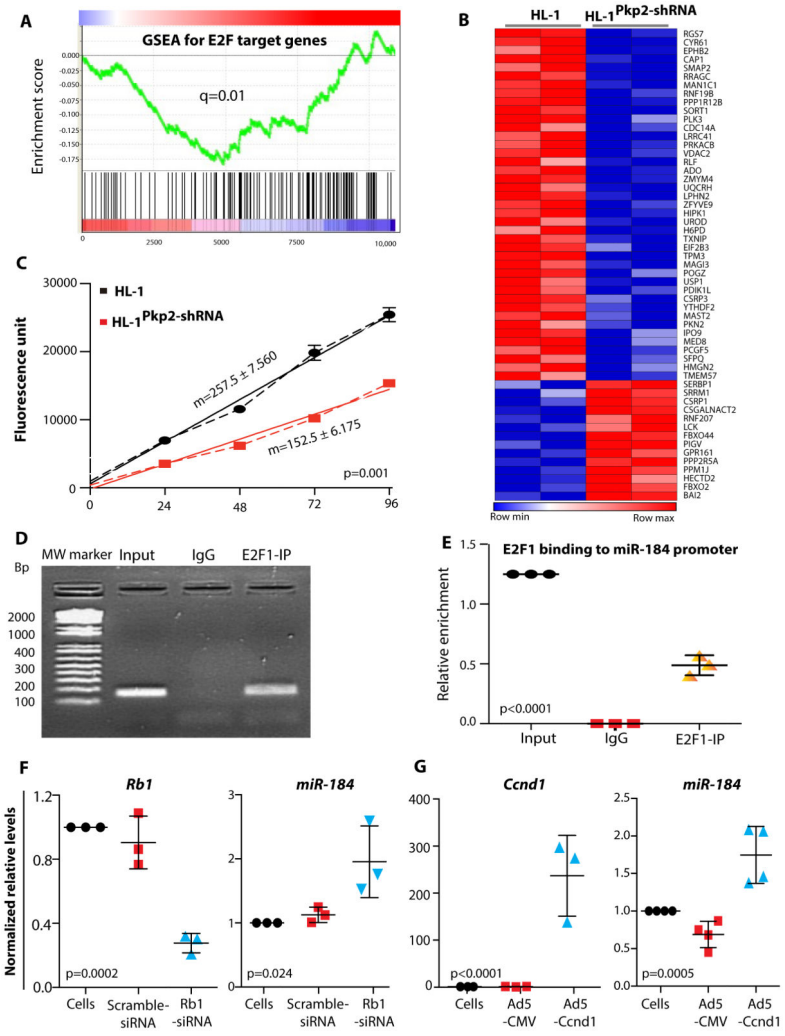

Figure 4. Regulation of miR-184 levels by E2F1 transcription factor

A) Gene Set Enrichment Analysis (GSEA) of the differentially expressed transcripts between wild type HL-1 and HL-1$^{Pkp2\text{-}shRNA}$ cells showing a significant enrichment of the E2F1 target genes. **B)** Heat map of E2F enrichment profile showing the predominantly downregulated transcripts (false discovery rate (FDR) is set at 0.01). **C**) Proliferation rate of wild type and HL-1$^{Pkp2\text{-}shRNA}$ cells, as determined by CellTiter Blue assay. Dotted lines show the growth curves at 4 different time points and straight lines the linear regression fit depicting slope of each curve (m value). **D**) Agarose gel electrophoresis photograph showing a 160 bp miR-184 5' genomic region amplified following precipitation of DNA with an anti E2F1 antibody in a ChIP assay. **E**) Quantitative data showing precipitated 5' genomic region of miR-184 relative to input in the ChIP assay. **F**) Rescue of miR-184 levels upon siRNA-mediated knock down of RB1 in HL-1 cells. Cells treated with a scrambled siRNA are included as controls. As shown *Rb1* transcript levels were reduced by 3.7 ± 0.6 –fold compared to control non-transfected cells (N=3 per group, p=0.0002). Panel to the right depicts increased miR-184 levels by 1.95±0.56 upon knock down of *Rb1* (N=3, p=0.024). **G**) Rescue of miR-184 upon over-expression of CCND1, which activates the E2F1 pathway and inactivates RB upon phosphorylation by CDK4/6. Levels of *Ccnd1* mRNA were

increased by 236±85 -fold upon transduction of HL-1 cells with recombinant adenoviruses, as shown in the graph to the left (N=3, $p<0.001$). In accord with increased *Ccnd1* levels, miR184 levels were changed in a similar direction and increased by 1.74± 0.38 -fold (N=4, $p=0.005$).

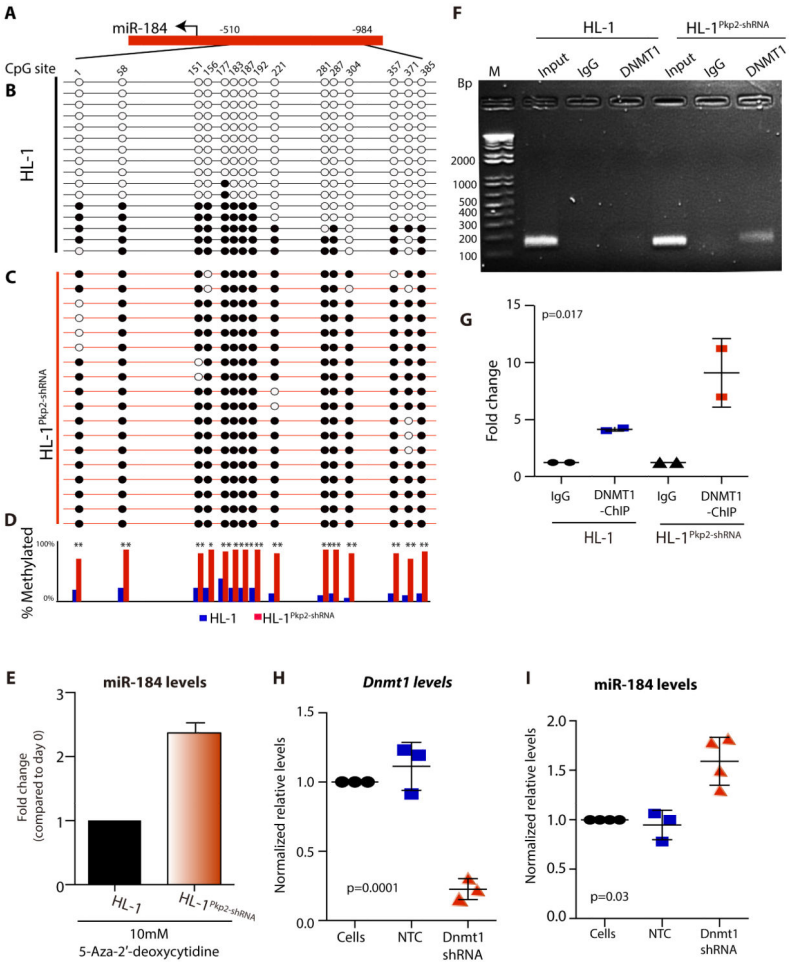

Figure 5. Epigenetic regulation of miR-184 in AC

A) Position of the CpG sites at the upstream regulatory genomic locus of miR-184. **B and C.** Analysis of DNA methylation at the mouse miR-184 locus by sodium bisulfite treatment and sequencing of PCR clones from HL-1 (**5B**) and HL-1$^{Pkp2\text{-}shRNA}$ cells (5**C**). Each row represents CpG methylation status of a randomly selected independent clone. **D)** Bar graph showing percent methylation of all CpG site in HL-1 and HL-1$^{Pkp2\text{-}shRNA}$ cells. All analyzed CpG sites show significant hypermethylation in the HL-1$^{Pkp2\text{-}shRNA}$ cells as compared to HL-1 cells alone (*p<0.01 and **p<0.001). **E)** Effects of treatment of HL-1 and HL-1$^{Pkp2\text{-}shRNA}$ cells with 10μm 5-aza-2′-deoxycytidine (5-azaD) on miR-184 levels determined daily. MiR-184 levels were increased after treatment with 5-azaD in both HL-1 and HL-1$^{Pkp2\text{-}shRNA}$ cells at 5 days post aza-C treatment. Magnitude of the induction in the HL-1$^{Pkp2\text{-}shRNA}$ was greater than that in the HL-1 cells (N=3, p<0.01). **F**) Photograph of agarose gel showing precipitation and amplification of a 160 bp genomic region of miR-184 with an anti DNMT1 antibody in a ChIP assay. **G**) Quantitative data from ChIP assay showing binding and fold increase in miR-184 5' genomic region precipitated in ChIP assay (N=2). **H and I**) Rescue of miR-184 levels upon knock down of *Dnmt1* transcript by 4.5±1.4 –fold (N=3, p=0.0001) and **i**ncreased miR-184 levels (1.6±0.2 -fold, N=4, p=0.03) upon knock down of *Dnmt1* RNA.

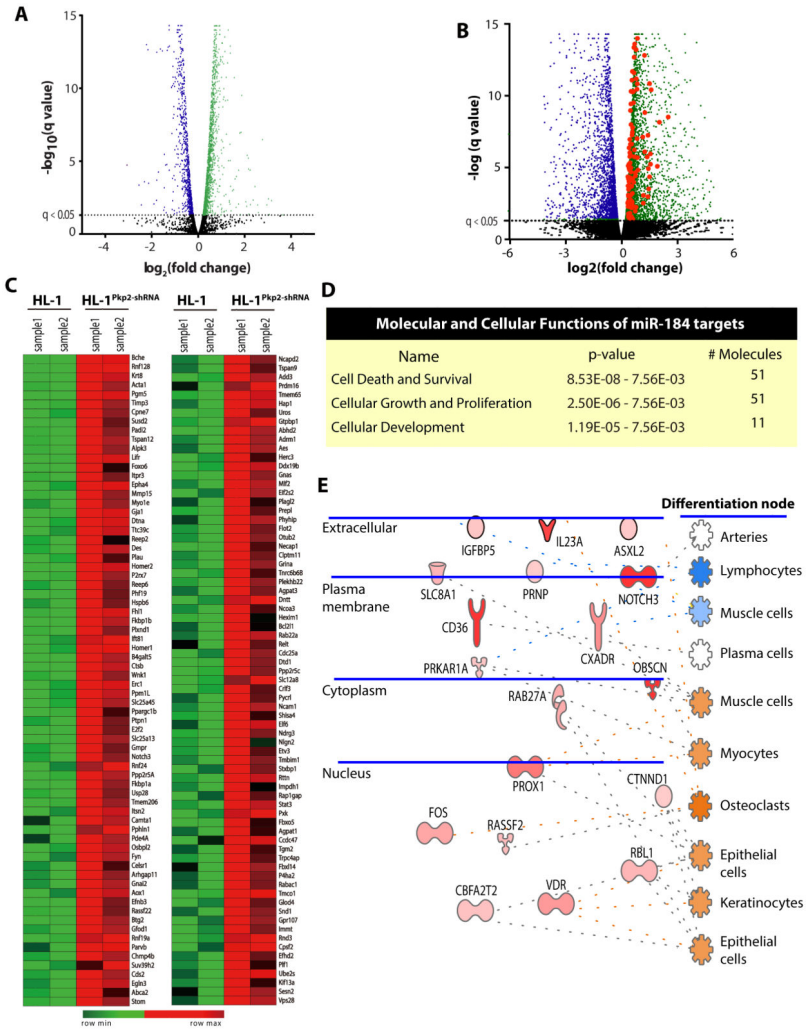

Figure 6. MiR-184:mRNA paired analysis

A) Volcano plot showing log2 fold change vs. −log10 q values for differentially expressed mRNAs levels as quantified by RNA sequencing from HL-1 and HL-1$^{Pkp2\text{-}shRNA}$ cells. The dotted line shows a q value of < 0.05. **B**) Volcano plot of differentially expressed miR-184 targets (red dots) superimposed on volcano plot of the differentially expressed transcripts showing miR-184 targets were upregulated in the HL-1$^{Pkp2\text{-}shRNA}$ cells. **C**) Heat plots of mRNA transcripts that were up regulated by more than 1.3-fold in HL-1$^{Pkp2\text{-}shRNA}$ cells and predicted to be the targets of miR-184 by at least 2 different target prediction programs. **D)** Prediction of molecular and cellular functions regulated by the miR-184 targets as determined by the Ingenuity Pathway Analysis (IPA). Top 3 functions are listed along with their corresponding p values and the number of affected genes. **E**) Gene network display from the IPA analysis of miR-184 targets showing the subcellular distribution and up regulation of miR-184 targets involved in cell differentiation.

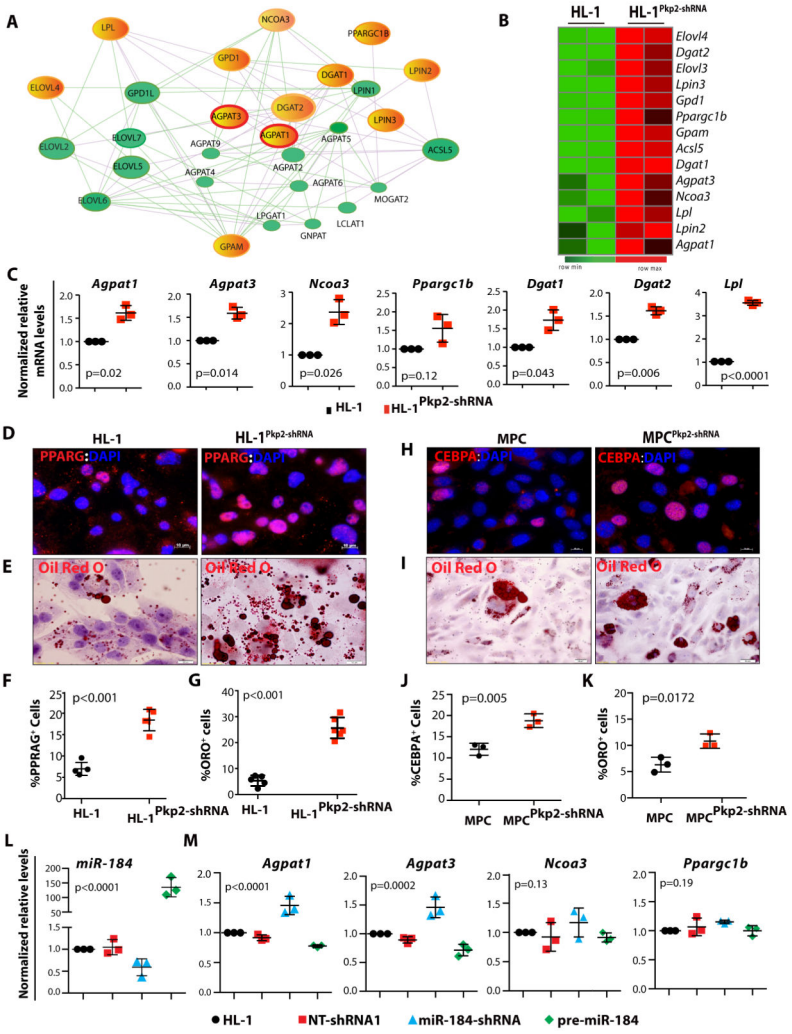

Figure 7. Adipogenic genes as targets of miR-184

Protein functional association network, constructed using STRING online tool for paired analysis of miR-184 and its mRNA transcripts involved in triglyceride synthesis, including *Agpat1, Agpat3, Ncoa3* and *Ppargc1b*. Genes directly targeted by miR-184 are highlighted as orange color. **B)** Heat plot constructed for paired analysis of miR-184 and its mRNA target networks involved in adipogenesis, which were upregulated in the HL-1$^{Pkp2\text{-}shRNA}$ cells. **C)** Confirmation of increased transcript levels of selected miR-184 targets involved in lipid metabolism (N=4) **D**) IF panels showing expression of nuclear PPARG, an adipogenic transcription factor, in the control HL-1 and HL-1$^{Pkp2\text{-}shRNA}$ cells 14 days after induction of adipogenesis. Corresponding (bottom panel) quantitative data, showing a 2.6±0.16 -fold increase in the number of PPARG expressing HL-1$^{Pkp2\text{-}shRNA}$, as compared to the control HL-1 cells (N=5, p<0.0001). **E)** Oil Red O stained panels showing increased lipid accumulation in the HL-1$^{Pkp2\text{-}shRNA}$ as compared to the control HL-1 cells 14 days after induction with an adipogenic medium (4.7± 0.4 -fold higher in the HL-1$^{Pkp2\text{-}shRNA}$, N=6, p<0.0001). **F, G)** Corresponding quantitative data, showing a 2.6±0.16 -fold increase in the number of PPARG expressing HL-1$^{Pkp2\text{-}shRNA}$ and 4.7± 0.4 -fold higher number of HL-1$^{Pkp2\text{-}shRNA}$ cells accumulating fat droplets, as compared to the control HL-1 cells (N=4,

p<0.0001 and N=6, p<0.0001, respectively). **H, I)** CEBPA expression and fat droplet accumulation in cardiac MPCs and MPCs knockdown for *Pkp2* ($MPC^{Pkp2\text{-}shRNA}$) after 5 days of adipogenic induction. **J)** Quantitative data showing 1.7±0.13 -fold increase in number of cells expressing adipogenic transcription factor CEBPA in the $MPC^{Pkp2\text{-}shRNA}$ cells, as compared to control MPCs (N=3,600 cells/group) **K)** Enhanced fat droplet accumulation (1.6±0.23 -fold) in $MPC^{Pkp2\text{-}shRNA}$ (N=3,800 cells/group) as compared to controls. **L)** Effects of knockdown and overexpression of miR-184 on selected target genes involved in adipogenesis. Transcript levels of *Agpat1* and *Agpat3* were increased by approximately 2-fold in HL-1 cells transduced with Lenti:$miR\text{-}184^{shRNA}$ as compared non-transduced HL-1 cells (N=3 per group, p<0.05). Conversely, over-expression of miR-184 was associated with about 25% decrease in the *Agpat1* and *Agpat3* mRNA levels (N=3, p=0.04), identifying these genes as the targets of miR-184. However, levels of *Ncoa3* and *Ppargc1b* were not changed upon over-expression or knock down of miR-184. To avoid potential confounding effects of the vector backbones, experiments were repeated with the viral constructs that had identical viral backbones in the control NT-shRNA, knock down and over-expression groups. Similar results were obtained for changes in the transcript levels of selected adipogenic markers in cardiac MPCs (Online Figure VII)

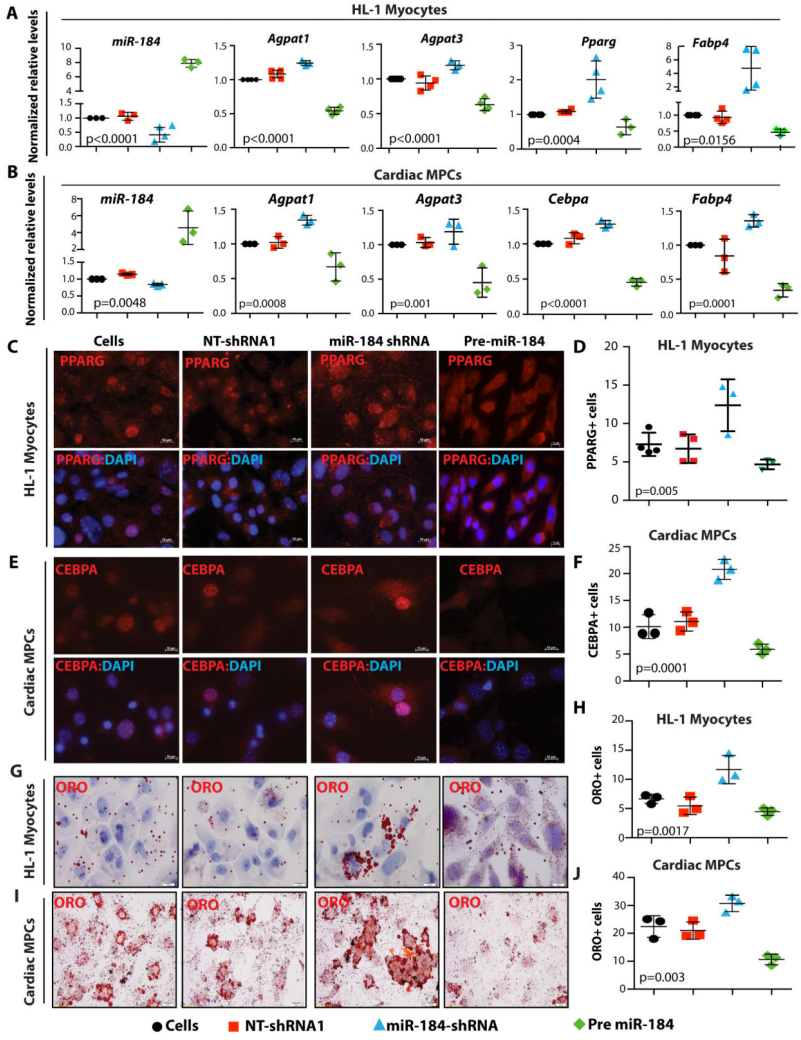

Figure 8. Effects of knockdown and over-expression of miR-184 on adipogenesis

A-D) Transcript levels of miR-184 and its targets showing knock down (Lenti:miR-184^{shRNA}) and over-expression (Lenti:*pre-miR-184*) of miR-184 in HL-1 cells and MPCs isolated from the heart. Levels normalized to non-transduced cells are presented as fold change. **A**) Transduction of HL-1 cells with Lenti:miR-184^{shRNA} construct leading to increased transcript levels of several adipogenic genes (*Pparg:* 2.15±0.56, p<0.05; *Fabp4:* 4.1±3.1, p<0.05; *Agpat*1: 1.3±0.1, p<0.001; and *Agpat3:* 1.2±0.1, p=0.007), as compared to control or the Lenti:NT^{shRNA} groups. In contrast, over-expression of miR-184, upon transduction of HL-1 cells with Lenti:*pre-miR-184*, was associated with decreased transcript levels of the adipogenic genes **B**) Over-expression and knock down of miR-184 levels in cardiac MPCs led to changes in the transcript levels of the selected miR-184 target genes, similar to those observed in the HL-1 cells. **C,D**) IF panels showing staining of adipogenic transcription factor PPARG and the corresponding quantitation data in HL-1 cells. The number of HL-1 cells expressing PPARG was increased by 1.8 ± 0.4 fold in the Lenti:miR-184^{shRNA} group, as compared to the control groups. In contrast, over-expression of miR-184 was associated with reduced number of HL-1 cells expressing PPARG (average

of 200 cells per group, N=3-4, p<0.05). **E, F**) IF panels show staining for CEBPA and the corresponding quantitative data in cardiac MPCs. The number of CEBPA expressing MPCs was increased upon knock down of miR-184 (2.03±0.18 fold, N=3, p=0.0002) and decreased upon over-expression of miR-184 (~ 200 cells per group, 1.74±0.27 fold N=3, p=0.046). **G, H**) Representative ORO-stained panels and the corresponding quantitative showing increased and decreased number of cells accumulating fat droplets in HL-1 cells transduced with Lenti:*miR-184*^{shRNA} and Lenti:*pre-miR-184*, respectively, as compared to the control groups (250 cells per group; N=3, p<0.05). **I, J)** Knock down and over-expression of miR-184 in MPCs was associated with increase (1.35±0.13 -fold, N=3, p=0.02) and decrease (2.2±0.4, N=3, p=0.004) fat droplet accumulation, respectively.

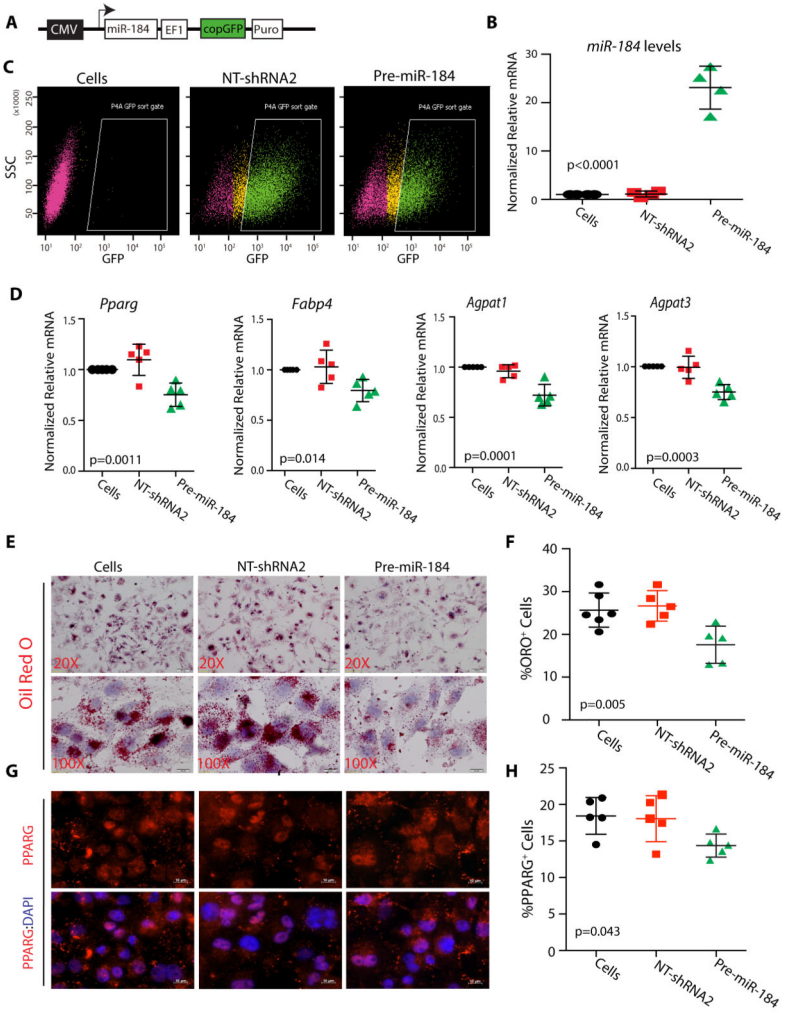

Figure 9. Attenuation of adipogenesis upon overexpression of miR-184 in the HL-1$^{Pkp2\text{-}shRNA}$ cells

A) Schematic of Pre-miR-184 expression construct showing expression regulation of miR by the CMV promoter and GFP by the EF1 promoter. **B)** Flow cytometry plot depicting GFP expressing in HL-1$^{Pkp2\text{-}shRNA}$ cells transduced with Non-targeting control (NT-shRNA2) or Lenti:pre-miR-184 viruses. **C)** QPCR analysis of miR-184 levels in HL-1$^{Pkp2\text{-}shRNA}$ cells transduced with Lenti:pre-miR-184 (N=3, p<0.0001). **D)** Reduced mRNA levels of *Pparg (27±10%)*, *Fabp4 (25±12%), Agpat1 (26*±13%) and *Agpat3 (25±9%)* in the HL-1$^{Pkp2\text{-}shRNA}$ cells transduced with Lenti:pre-miR-184, as compared to the control groups (N=5, p<0.05). **E and F)** Reduced accumulation of fat droplets upon overexpression of miR-184 (Lenti:*pre-miR-184*) as detected by Oil Red O (**E**) and the corresponding quantitative data (**F**). **G-H)** IF staining and quantitation of cells expressing PPARG in the experimental groups (N=5, p=0.043).